

HORNBLLENDE-BIOTITE ELEMENT PARTITION

IN THE LOON LAKE AUREOLE

---

ELEMENT PARTITION BETWEEN HORNBLLENDE AND BIOTITE IN THE ROCKS FROM  
LOON LAKE AUREOLE, CHANDOS TOWNSHIP, ONTARIO

By  
MING CHEN CHIANG, B.S..

A Thesis  
Submitted to the Faculty of Graduate Studies  
in Partial Fulfilment of the Requirements  
for the Degree  
Master of Science

McMaster University

December, 1965

MASTER OF SCIENCE (1965)  
(Geology)

McMASTER UNIVERSITY  
Hamilton, Ontario

TITLE: Element Partition Between Hornblende and Biotite in the Rocks  
from Loon Lake Aureole, Chandos Township, Ontario

AUTHOR: Ming Chen Chiang, B.S. (National Taiwan University)

SUPERVISOR: Professor D. M. Shaw

NUMBER OF PAGES: viii, 83.

SCOPE AND CONTENTS: The geology of the northeastern and southwestern sections of the aureole of the Loon Lake pluton of Chandos township was mapped. Thirty five pairs of hornblende and biotite were separated from the rocks and spectrographically analyzed for Be, Ga, Ti, Cr, V, Li, Ni, Co, Cu, Mn, Zr, Sr, Ba and Rb. Major element analyses were made by wet chemical methods on 8 pairs of hornblende and biotite. The relations of minor and major elements are discussed in terms of distribution coefficients.

#### ABSTRACT

Spectrographic analyses of Be, Ga, Ti, Cr, V, Li, Ni, Co, Cu, Mn, Sr, Zr, Ba, and Rb for 35 hornblende-biotite pairs, and wet chemical analyses of major elements for 8 pairs, were made for rocks from the aureole of the Loon Lake pluton in Chandos township, Ontario. Distribution coefficients,  $D = X_A^{\text{Hb}} / X_A^{\text{Bio}}$ , for major and minor elements were calculated. D values are nearly constant for Si, Al, Fe, Mg, K, Be, Cr, V, Li, Ni, Co and Mn, but variations<sup>are</sup> observed, which cannot be related to the temperature variation during metamorphism. Erratic D values were found for Na, Ca, Ga, Ti, Cu, Zr, Sr and Rb. A minor element shows geochemical coherence with a major element when the distribution coefficients are similar.

## TABLE OF CONTENTS

	Page
INTRODUCTION	1
ACKNOWLEDGMENTS	1
GENERAL GEOLOGY	3
Definition of Terms	3
Igneous Rocks - syenite, diorite, granitic rocks	6
Amphibolite	8
Metasedimentary Rocks - marble, paragneiss	10
Structural Geology	11
METAMORPHISM	13
Regional Metamorphism	13
Contact Metamorphism - hornblende hornfels facies, pyroxene hornfels facies	17
ELEMENT PARTITION BETWEEN HORNBLLENDE AND BIOTITE	24
Introduction	24
Review of Previous Work	24
Analytical Methods	29
Mineral Composition and Calculation of Molecular Formula	32
MAJOR ELEMENT DISTRIBUTION BETWEEN HORNBLLENDE AND BIOTITE	35
MINOR ELEMENT DISTRIBUTION BETWEEN HORNBLLENDE AND BIOTITE	42
Minor Elements in Tetrahedral Coordination	43
Minor Elements in Octahedral Coordination	46
Minor Elements in 8- or 12-fold Coordination	54

	Page
SUMMARY	62
REFERENCES	64
APPENDICES	68

## LIST OF TABLES

Table	Page
1. G-1 and W-1 analyses	31
2. Variation coefficient of spectrographic analyses	31
3. Values of K and D for major elements	41
4. Distribution coefficients (D), ionic radii (r), and electronegativities (e), of cations in tetrahedral coordination	43
5. Distribution coefficients (D), ionic radii (r), and electronegativities (e) of cations in octahedral coordination	46
6. Distribution coefficients (D), ionic radii (r) and electronegativities (e) of cations in 8- or 12-fold coordination	54

LIST OF FIGURES

Figure	Page
1. Generalized geological map of Loon Lake pluton, and its vicinity, Chandos township, county of Peterborough, Ontario.	4
2. ACF diagram of the almandine amphibolite facies	15
3. ACF diagram of the hornblende hornfels facies	20
4. ACF diagram of the pyroxene hornfels facies	22
5. Distribution of Be between hornblende and biotite )	
6. Distribution of Ga between hornblende and biotite )	45
7. Distribution of Ti between hornblende and biotite )	
8. Distribution of Cr between hornblende and biotite )	48
9. Distribution of V between hornblende and biotite )	
10. Distribution of Li between hornblende and biotite )	50
11. Distribution of Ni between hornblende and biotite )	
12. Distribution of Co between hornblende and biotite )	51
13. Distribution of Cu between hornblende and biotite )	
14. Distribution of Mn between hornblende and biotite )	53
15. Distribution of Zr between hornblende and biotite )	
16. Distribution of Sr between hornblende and biotite )	55
17. Distribution of Ba between hornblende and biotite )	
18. Distribution of Rb between hornblende and biotite )	57
19. Relation of distribution coefficients and metamorphic grades	59-61

## APPENDICES

	Page
1. Mineral composition and approximate mode of samples	68
2. Detail of the spectrographic method	73
3. Analytical and standard spectral lines, and the range of working curves	75
4. Chemical analyses	76
5. Spectrographic analyses	80

## INTRODUCTION

Major and minor element distribution between coexisting minerals has been considered by many authors. Kretz (1959) and Moxham (1965) studied the relationships of elements in coexisting hornblende and biotite with respect to the metamorphic state of the rocks, but the behaviour of minor elements in coexisting minerals is dependent on temperature or other factors and could not be explained satisfactorily.

The present attempt at solution of these problems involved the use of wet chemical analyses for major elements and a spectrographic method for the minor elements of hornblende and biotite in rocks from the contact aureole of the Loon Lake pluton and nearby. The temperature of the rocks in the contact aureole is believed to have increased toward the intrusive pluton, so study of element partition between coexisting minerals in the metasedimentary rocks collected between the outside of the contact aureole and inwards to the intrusive body or inclusions in the igneous rocks, might solve the question of whether the distribution coefficient changes significantly in response to temperature.

The present attempt to interpret the behaviour of minor element is made in the light of mineral structures and the distribution coefficients of both major and minor elements.

## ACKNOWLEDGEMENTS

I wish to express my thanks to Professor D.M. Shaw for his suggestion of this topic and assistance during the investigation; also to

Dr. H.P. Schwarcz for his guidance both in the field and laboratory.

I would like to express my gratitude and appreciation to G.E. Pattenden for his valuable assistance with the spectrographic analytical work, and to fellow graduate students, especially P.A.M. Anderson, for advice and discussion during this research, and J. Payne for contribution of a nepheline-syenite sample.

## GENERAL GEOLOGY

Previous Work The general geology of Chandos township, Peterborough county, Ontario, was first mapped by Adams and Barlow (1910), and later amended by Hewitt and Satterly (1957) in their Map No. 1957b which covers the Haliburton-Bancroft area. Shaw mapped the Chandos area on the scale of one inch to two miles and his report (1962) has been used as the base map for the present work. The Loon Lake pluton was studied by Cloos (1934) and Saha (1959).

Present Work In the summer of 1964, the author spent three weeks mapping the northeastern and southern part of the contact aureole of the Loon Lake pluton using four inches to one mile aerial photographs. Since the eastern part of the area is a swamp and the northwestern boundary of the intrusive body is not clear, these areas were not studied. A generalized geological map of the region, indicating the collecting areas, is given in Fig. 1.

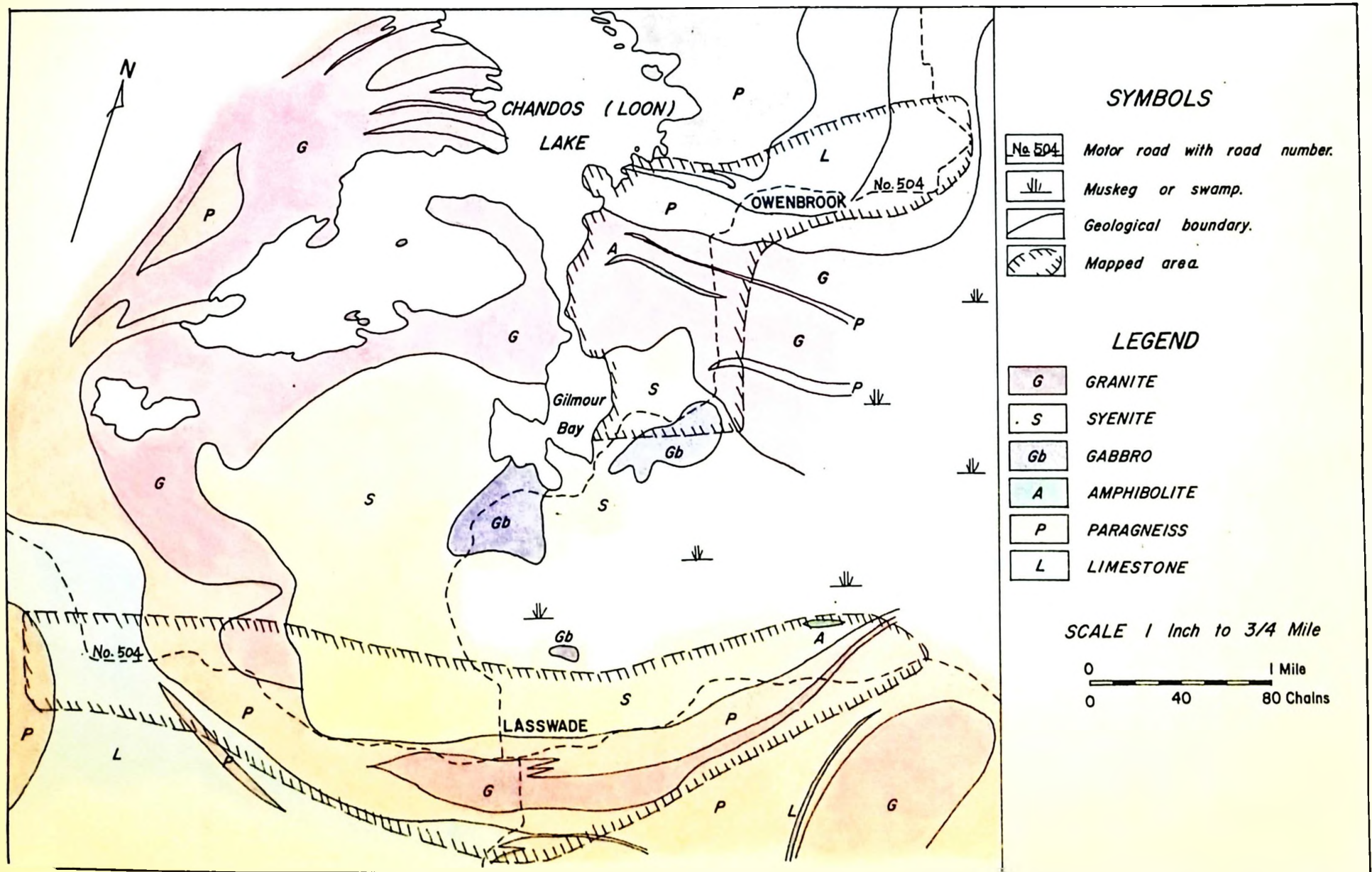
### Definition of Terms

The following terms used in this paper are taken from those listed by Shaw (1957).

Grain size definitions: Fine grain, less than 1 mm; medium grain, 1 to 5 mm; coarse grain, greater than 5 mm.

Amphibolite: A metamorphic rock of medium to coarse grain, containing essential amphibole and plagioclase. Amphibolites are commonly massive

Fig. 1 GENERALIZED GEOLOGICAL MAP OF LOON LAKE PLUTON, AND ITS VICINITY,  
 CHANDOS TOWNSHIP, COUNTY OF PETERBOROUGH, ONTARIO



and the amphibole often has an elongated or acicular habit, but some varieties can be classed as schist or gneiss. Many amphibolites also contain pyroxene, mica, epidote, or garnet and can be prefixed accordingly. Quartz is also a common constituent.

Ortho-amphibolite: An amphibolite derived from igneous rock.

Para-amphibolite: An amphibolite derived from sedimentary rock.

Gneiss: A rock possessing gneissosity. The directions of easiest fracture may be parallel or transverse to the layering but parallel cleavage is less regular than schists. Granular (equi-dimensional) minerals such as quartz, feldspar, garnet commonly predominate, but mica, amphibole, pyroxene, and other silicates contribute to the foliation or lineation. Invariably it is a rock of medium or high metamorphic grade and usually rather inhomogeneous.

Orthogneiss: A gneiss of igneous origin.

Paragneiss: A gneiss derived from a sedimentary rock.

Lit-par-lit gneiss: A mixed gneiss with regular alternation of quartzofeldspathic (granitic) and mafic layers.

Granite: A rock of medium or coarse grain size, containing essential quartz and alkali feldspar. The term is commonly applied in the field to rocks where the composition of the feldspar is uncertain. Usually massive with regular interlocking texture.

Hornfels: A recrystallized rock of fine or medium grain produced by contact metamorphism. Schistosity and slaty cleavage are absent and a hornfels is usually composed of a mosaic of equidimensional grains without preferred orientation. Fine-grained varieties commonly have a conchoidal fracture. Porphyroblasts may be present. The name is chiefly applied to pelitic rocks but is used for others where appropriate. In some cases it is used as a purely descriptive term, not necessarily implying a product of contact metamorphism.

Marble: A metamorphic rock composed mainly of calcite or dolomite.

Migmatite: A mixed rock partly consisting of quartzo-feldspathic (granitic) material, together with older metamorphosed rock. Migmatites are commonly gneissic but not necessarily so.

### Igneous Rocks

The igneous rocks that form the Loon Lake pluton, consist of syenite, diorite and granitic rocks. The author did not study these rocks in detail and the following brief statement was in part taken from Saha's (1959) work.

#### Syenite

The syenite making up the main body of the Chandos pluton is a pinkish, massive, medium- to coarse-grained rock, consisting of plagioclase ( $An_{30\pm3}$ ), microcline, microperthite and biotite, with accessory hornblende sphene, calcite, quartz and magnetite. It differs from granite by the absence of megascopically visible quartz.

Potash feldspar is the most abundant mineral making up about half of the rock: it gives the rock a pinkish colour and increases in amount towards the edge of the pluton. Plagioclase amounts to about 40%. The main mafic mineral amounting to about 5% is biotite, some of which has altered to chlorite on the margin.

Saha (1959) concludes that the syenite tends to become more silicic from the center towards the margin of the body, accompanied by an increase in the potassium content and a decrease in mafic minerals, plagioclase, and the anorthite content of plagioclase feldspar.

#### Diorite

Dark, massive diorite occurs in the syenite body near Gilmour Bay. Abundant very coarse-grained, gray to brownish-gray plagioclase ( $An_{30-35}$ ) and dark biotite are megascopically evident. Hornblende, quartz, sphene and opaque minerals (magnetite, etc.) are also present. Bending of cleavage and twinning planes of crystals of biotite and plagioclase was seen under the microscope, and was presumably the result of non-hydrostatic stress after crystallization of the rock. Plagioclase feldspar makes up more than 60% of the rock, the remainder including 25% biotite and 10% hornblende. The last forms sieve-like aggregates of small crystals developed at the expense of other ferromagnesian minerals, and some grains show alteration to mica.

Small, clear, untwinned plagioclase grains occur interstitially to the strained larger crystals. This, together with the different orientation of quartz, indicates partial recrystallization after shearing.

### Granitic Rocks

The granitic rocks include granodiorite, granite, aplite and pegmatite. Granodiorite may be followed gradually to granite and the boundary is not easily defined. Aplite and pegmatite outcrops are too small to show on the map. The author tentatively grouped all these rocks for mapping into one unit which differs from syenite by having the quartz observable in the field.

Specimens are gray, pink or reddish brown, medium- to very coarse-grained, with or without gneissic structure. The essential minerals are quartz, plagioclase ( $An_{10-30}$ ), microcline, biotite, and hornblende, commonly with accessory magnetite, sphene, calcite, apatite, zircon, tourmaline and pyrite.

Granitic rocks are more abundant in the outermost parts of the pluton. In addition, elongated granitic bodies occur parallel to the strike of the paragneiss in both the north and the south parts of the pluton. Commonly, they contain inclusions of paragneiss, of lit-par-lit gneiss or migmatite. Numerous irregular pegmatite veins are very common in marble areas.

### Amphibolite

This is a dark, massive rock, containing more than 50% of hornblende and showing fairly homogeneous mineralogical composition in the outcrops. Gneissic structure is obscure, foliation is not easy to observe and some rocks show hornfelsic texture. These rocks form elongated bodies usually enclosed in igneous rocks or marble, and are believed (Shaw, 1962) to have been derived from igneous rocks, but this needs further study to be sure.

About one mile northeast of Gilmour Bay, one such body, 200 feet wide, 3000 feet long is enclosed in granitic rocks. It is massive, consisting mainly of hornblende and plagioclase ( $An_{35-40}$ ), with subordinate biotite and quartz; accessory sphene, calcite and magnetite are common. Penetrating pegmatic veins are common, and usually consist of very coarse-grained plagioclase, quartz, pinkish microcline and a little magnetite showing good octahedral outlines.

Two miles northeast from Lasswade, there is another amphibolite body, 2000 feet long and 150 feet wide, trending east-west and enclosed in syenite. Foliation and gneissic structure are absent but numerous syenite veins from an inch to a few feet wide penetrate from the country rocks into the amphibolite and in places it becomes migmatitic near to the contact. The amphibolite is dark, coarse to very coarse-grained, homogeneous, massive rock, consisting predominantly of hornblende, less diopside, plagioclase ( $An_{40-45}$ ), and quartz. Plagioclase sometimes shows bending of cleavage and twinning planes. Diopside has commonly altered to hornblende along the rim or along the cleavage. In some part were found hornblende crystals one to two inches long with a few quartz crystals. The accessory minerals are commonly biotite, magnetite, pyrite and sphene.

About two and a half miles west of Lasswade in the marble area, there are two small amphibolite bodies, a few hundred feet long and about 30 feet wide, consisting mainly of hornblende, pyroxene, biotite, plagioclase and quartz.

## Metasedimentary Rocks

### Marble

This is a white, gray to dark gray, coarse-grained rock containing more than 50% calcite, with or without foliation, which results from the presence of other minerals such as biotite and tremolite. Marble is very commonly interbedded with biotite-paragneiss or para-amphibolite in this area. Lamination structure formed by the alternation of thin biotite-rich and calcite-rich layers is very common. Sometimes the biotite-rich layer is thicker, and may be mapped as a biotite-paragneiss unit, often sheared out into boudins enclosed in marble. These are very commonly observed about a half mile south of Lasswade, but dragfolds or distorted bedding are very rarely found. To the west of Lasswade, the marble contains numerous pegmatite veins irregularly distributed through the whole area.

The marble occurring to the northeast of Gilmour Bay is coarser in grain size and has more amphibole, mica and scapolite than that to the west of Lasswade. This may suggest that the original impure limestones did not have the same chemical composition.

### Paragneiss

The area of paragneiss was mapped by Shaw (1962) as para-amphibolite, consisting predominantly of amphibole but also containing essential plagioclase. The present author failed to find para-amphibolite in this area, for although some thin layers of paragneiss do contain more than 50% of amphibole, in the majority amphibole is not the predominating constituent and commonly is an accessory mineral or even absent; likewise, plagioclase is not always an essential mineral in some rocks.

The essential minerals in these rocks include biotite, diopside, hornblende, garnet, hypersthene, allanite, uranite, scapolite, epidote, plagioclase, microcline, and quartz; accessory calcite, sphene, muscovite, magnetite, pyrite, ilmenite, zircon, tourmaline, cordierite and apatite are common. The mineral assemblage varies from layer to layer, the commonest being biotite-plagioclase-quartz and hornblende-diopside-biotite-plagioclase-quartz in thin layer alternation. The biotite-rich part was more easily weathered, becoming rusty if a few pyrite grains were present in the rock.

Near the contact of the syenite pluton, the rock becomes hornfelsic, and foliation planes and lineations are less pronounced. Numerous injections of igneous material, thin or thick, intimately penetrate into the paragneiss body along the fabric planes, and the rock becomes migmatitic where the igneous part dominates. This is very often the case along the southern border of the pluton. In addition, there are many lens-like paragneiss bodies enclosed in the syenite. The trends of these lenses are roughly parallel to the contact and to the strike of the paragneiss which becomes steeper in dip nearer to the contact. More detailed discussion of the petrography of the paragneiss will be found in the following chapter.

#### Structural Geology

The structure of the Loon Lake pluton has been studied by Cloos (1934) and Saha (1959), and the general structural geology of the Chandos township has been described by Shaw (1962).

The ovoid shape of the pluton is like a funnel steeply plunging to east with walls dipping inward from all sides at angles of  $70^{\circ}$  -  $80^{\circ}$ . The diorite-gabbro bodies near Gilmour Bay represent the centre of upwelling of a magmatic mush, and possibly the downward extension of their positions represents the locations of the vents through which the magma came up and extended outward. The surrounding metasedimentary rocks dip toward the centre of the pluton and are, in general, conformable to the margin of the intrusive rocks, becoming steeper or vertical nearer to the contact.

In the light of his data, Saha (1959) interprets the development of the Loon Lake complex as follows. The pluton was emplaced at the close of the earth movements which folded and metamorphosed the Grenville sediments by forceful upward and outward injections along the foliation planes of paragneiss; fractional crystallization and partial assimilation of inclusions followed these injections, which forced apart the walls and produced contact metamorphism of inclusions and country rocks.

## METAMORPHISM

The sedimentary rocks of this area were metamorphosed during two periods, according to Shaw (1962); first by regional metamorphism, and later by the intrusion of the Loon Lake pluton, which superimposed a contact metamorphic aureole on the nearby rocks. However, metamorphic processes are so complicated that the temperatures and pressures are uncertain, especially since the granitic and syenitic magmas contained an uncertain amount of water, which could play an important role during contact metamorphism. Therefore, the rocks in the contact aureole were metamorphosed not only by increasing temperature, but also by changing load pressure,  $P_{H_2O}$ , and probably  $P_{CO_2}$ .

### Regional Metamorphism

During regional metamorphism, the paragneiss and marble in this area were raised to the almandine amphibolite facies, as indicated by their mineral assemblages (see Appendix 1). It is not easy here to define subfacies or subzones of the almandine amphibolite facies, since the original rocks (impure limestone, calcareous or arenaceous sediments) were poor in aluminum, and do not contain diagnostic aluminum silicate minerals such as sillimanite, andalusite, kyanite, or staurolite.

The mineral assemblages of the specimens collected are shown in Appendix 1. Using the same sample numbers as appear on geological maps in the envelope, the various mineral assemblages are listed as follows (in order of decreasing abundance).

No. of Sample	Mineral assemblages (minerals in brackets are accessories)
712, 713	q-bio-mc-(mt-pl)*
717	q-bio-g-mc-(muc-mt-ap)
508	q-bio-pl(An <sub>37</sub> )-mc-hb-(cal-mt)
501, 503, 747, 758-4, 761, 770, 780, 781, 782, 786	q-bio-pl(An <sub>25-40</sub> )-hb-(cal-sp-mt)
703, 705, 711, 715	bio-q-hb-scp-pl(An <sub>35-45</sub> )-(mt)
788	mc-q-bio-hb-scp-(sp-mt)
789	q-bio-hb-ep-(cal-sp)
710	q-dio-hb-scp-(bio)
709	dio-scp-q-(sp-mt-pyt)

\* Abbreviation of minerals are listed in Appendix 1.

The above mineral assemblages are illustrated in the ACF diagram in Fig. 2, note that most of the samples contain hornblende and biotite. The following are polyphase assemblages and probably indicate disequilibrium, or presence of additional components, and are not shown in the ACF diagram.

707	q-hb-scp-ep-(cal-sp-mt)
708	q-scp-dio-bio-(hb-mt-sp-ap)
757	scp-dio-hb-bio-pl-(cal)

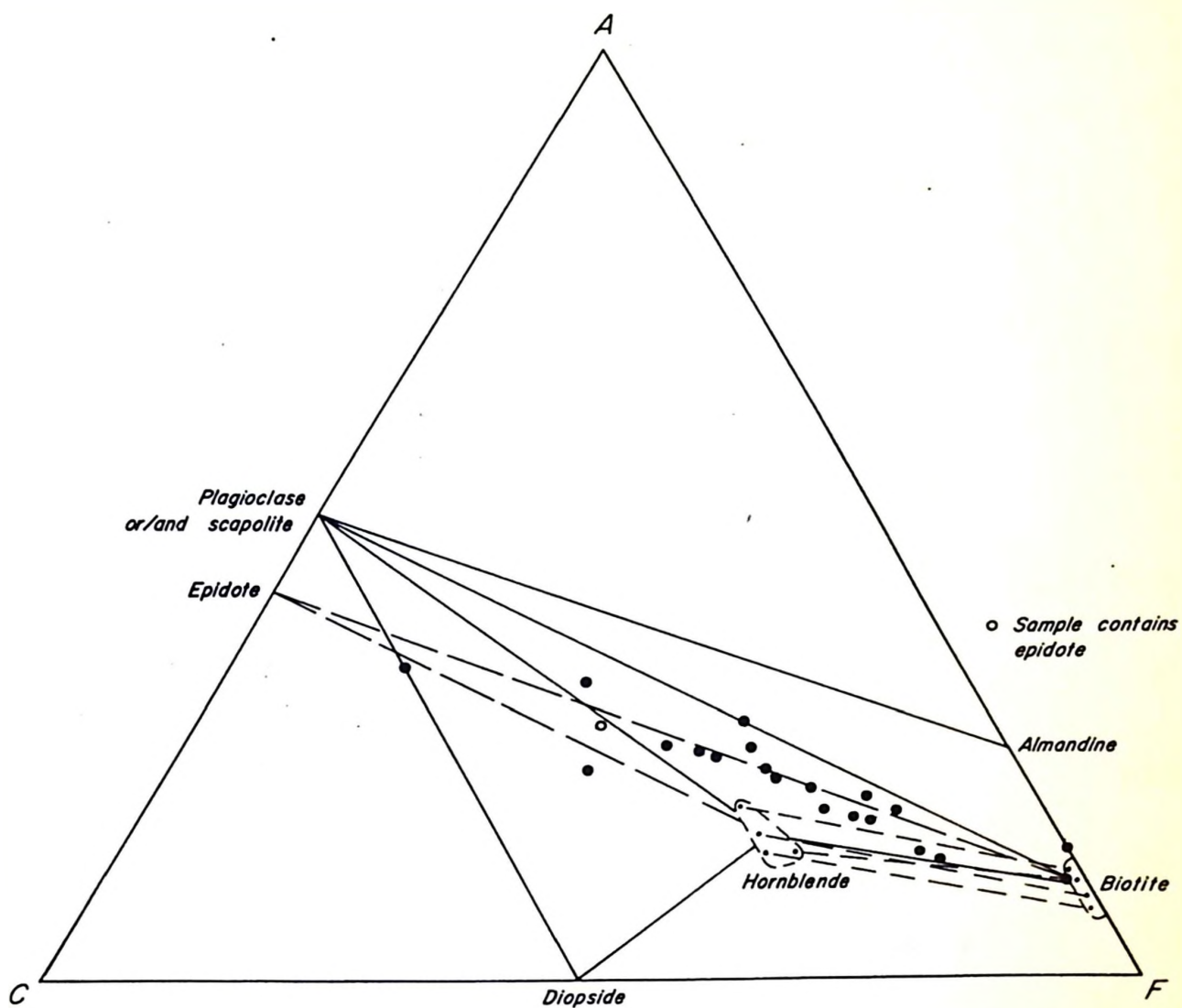


*Fig. 2 ACF diagram of the almandine amphibolite facies. Positions of hornblende and biotite are based upon wet chemical analyses. (Modified from Fyfe, Turner and Verhoogen, 1958, Fig. 105.)*

Quartz is the dominant mineral, commonly comprising more than 50% of the rocks. Scapolite is found in a wide variety of metamorphic rocks, and its abundance may be attributed to the presence of chlorine and sulfur. Hypersthene in rock No. 758-4 is a relic mineral, and most of it has altered to hornblende. Epidote was found not only in these regionally metamorphosed rocks, but also in the contact aureole. Amphibole is well developed and sometimes becomes dominant.

Although epidote is abundant in some rocks, these rocks do not fit the definition of the epidote amphibolite facies, owing to the presence here of oligoclase or andesine instead of albite. Some hand-specimens also contain a certain amount of garnet, and may be classified in the almandine amphibolite facies. Shaw (1962) found an outcrop containing sillimanite and cordierite at the beach west of Owenbrook, and another containing sillimanite and staurolite, one and a half miles east of Owenbrook. Staurolite may be a relic mineral and cordierite can be found even in the rocks formed by regional metamorphism (Hietanen, 1956). Thus one may conclude that the rocks near Owenbrook have some of the characteristics of the sillimanite-almandine subfacies of the almandine amphibolite facies. However, in the southern part of the area, none of the characteristic aluminum silicate minerals was found. Although there is consequently some doubt whether the rocks of the whole area are in the same subfacies, nevertheless the metamorphic grade of the southern part may be tentatively placed also in the almandine amphibolite facies.

### Contact Metamorphism

Since the rocks were raised to a high regional metamorphic facies, the superimposed thermal effects of the intrusion of the pluton on these rocks are not everywhere clearly distinguishable. The presence of hornfelsic texture and the mineral assemblages of the paragneiss near to, or as inclusions in, the southern part of the intrusive body are the evidences of the contact metamorphism.

To the north, granitic rocks occur between syenite and paragneiss, which strikes roughly parallel to the outline of the igneous body. There is no recognizable contact feature found in the paragneiss or marble, and study of the rocks and thin sections confirms that the mineral assemblages of these rocks do not show any clear departures from the almandine-amphibolite facies. The occurrence of the cordierite-sillimanite assemblage which Shaw found at the beach west of Owenbrook was not necessarily formed by the thermal effects of the intrusion. The indistinct nature of the contact aureole in this part may be due to the lower temperature of granitic magma in contact with the paragneiss and marble.

Rocks having hornfelsic texture are often found on the southern sector of the aureole along highway No. 504 near Lasswade; they are commonly dark-gray colour, fine- to medium-grained, and sometimes contain epidote-rich patches. Gneissic texture and lineation are rare or absent. Occasionally, dragfolds are observed where the original sedimentary bedding is preserved. Two facies, hornblende hornfels facies and pyroxene hornfels facies, are recognizable.

1. Hornblende hornfels facies Rocks showing the hornfelsic texture of this facies are distinguished from the pyroxene hornfels facies by the absence of hypersthene, and of cordierite if potash-feldspar is present. Various mineral assemblages are listed below, the minerals being listed in order of decreasing abundance, using sample numbers as on the geological map.

No. of Sample	Mineral assemblages (minerals in brackets are accessories)
605	q-pl( $An_{37}$ )-bio-g-(mt-cal)*
719, 720, 750	q-pl( $An_{27}$ )-bio-mc-(cal-nt-sp)
604, 606, 607, 724, 727, 735, 739, 752(2), 753, 755	q-bio-hb-pl( $An_{33-5}$ )-(cal-nt-sp-il)
745, 749	q-hb-bio-(ep-pl-nt-sp-cal)
721	hb-q-pl( $An_{40}$ )-(sp)
605(2)	q-hb-aln-(mt-pl-sp)
506, 722, 736	q-hb-dio-pl( $An_{30-45}$ )-(bio-sp-nt)
728	q-dio-hb-(cal-sp-nt)
507, 741	q-dio-ep-hb-(pl-sp-nt)
725	q-dio-pl( $An_{45}$ )-(bio-nt-sp)

\* Abbreviation of minerals are listed in Appendix 1.

The above mineral assemblages are illustrated in Fig. 3. The following assemblages have more than one extra phase and are not shown in the ACF diagram.

No. of Sample	Mineral assemblages (minerals in brackets are accessories)
742	q-dio-hb-ep-scp-pl( $An_{36}$ )-(cal-nt-sp)
744	q-pl( $An_{38}$ )-hb-bio-ep-(sp)
752(1)	q-ep-g-hb-scp-(pl-cal-sp-nt)
756, 791	q-pl( $An_{32}$ )-bio-hb-ep-(cal)

Sphene is the accessory mineral found in most of the samples. Epidote is an essential mineral in some assemblages of both this facies and the almandine amphibolite facies. Previous work indicates that the epidote minerals form between 300° and 500°C (Ramberg, 1949; Stringham, 1952; Rosenqvist, 1952), and are stable in the greenschist facies and epidote-amphibolite facies and unstable in the almandine amphibolite facies (Harpum, 1954). In this area, this is not the case, the anomaly is only apparent; epidote minerals coexist with oligoclase or andesine, and the rocks usually contain accessory calcite, whereas, in the greenschist facies and epidote-amphibolite facies, epidote coexists with albite. That epidote becomes a dominant mineral in the hornblende hornfels facies may be due to temperature,  $P_{H_2O}$ , and bulk composition being favourable to its formation.

Sieve-like hornblende is very common in this facies, the inclusions being usually quartz, occasionally magnetite and sphene, and rarely, plagioclase. This kind of hornblende probably formed at the expense of some ferromagnesian minerals, the excess silica being preserved as inclusions. Decolourized hornblende is occasionally observed, green or brownish-green hornblende becoming colourless along its cleavages or at edges of the crystal. This becomes more obvious if the hornblende crystal is close to

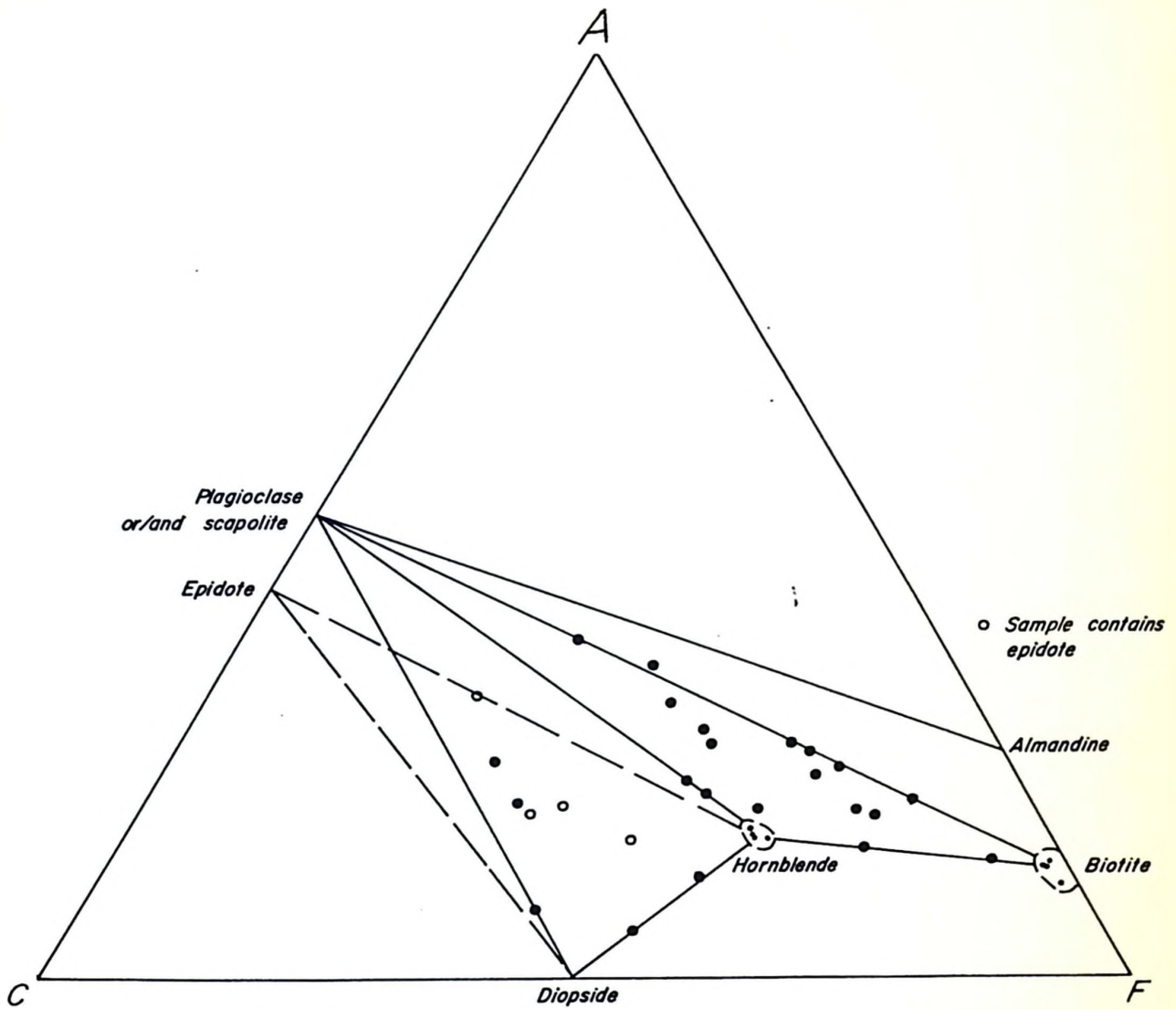


*Fig. 3 ACF diagram of the hornblende hornfels facies. Positions of hornblende and biotite are based upon wet chemical analyses. ( Modified from Fyfe, Turner and Verhoogen, 1958, Fig. 85 )*

one of the quartz veinlets which cut through the rock, and which may have brought in alkalis by hydrothermal solution to bleach the hornblende (Eose, 1959).

Plagioclase in this facies is mostly andesine ( $An_{30-40}$ ) with less oligoclase, both of which can coexist with scapolite or epidote, or even with both minerals (rocks No. 742, 744, 752, 756, and 791). The compositional relations between plagioclase, scapolite and epidote are uncertain at present.

2. Pyroxene hornfels facies The rocks of this facies occur as inclusions in syenite to the north of Lasswade, as shown on the geological map, and are distinguished from the hornblende hornfels facies by the common presence of hypersthene or cordierite. The following shows mineral assemblages identified by study of thin sections.

No. of Sample	Mineral assemblages (minerals in brackets are accessories)
504	di-scp-pl( $An_{45}$ )-q-(g-sp-mt)
603(1)	q-pl( $An_{37}$ )-bio-cord-(mt)
603(2)	hy-q-pl( $An_{37}$ )-bio(mt)
726	hy-q-pl( $An_{50}$ )-ura-(mt)
72-200-4	hy-q-pl( $An_{37}$ )-hb-(mt-bio)

The above mineral assemblages are illustrated in the ACF diagram (Fig. 4) and all of them are of sedimentary origin, having the relic bedding and mineralogical variation from layer to layer. Hypersthene is the characteristic mineral in these rocks, some of which contain nearly 10 per cent of magnetite or other iron oxides. There is, however, still a small

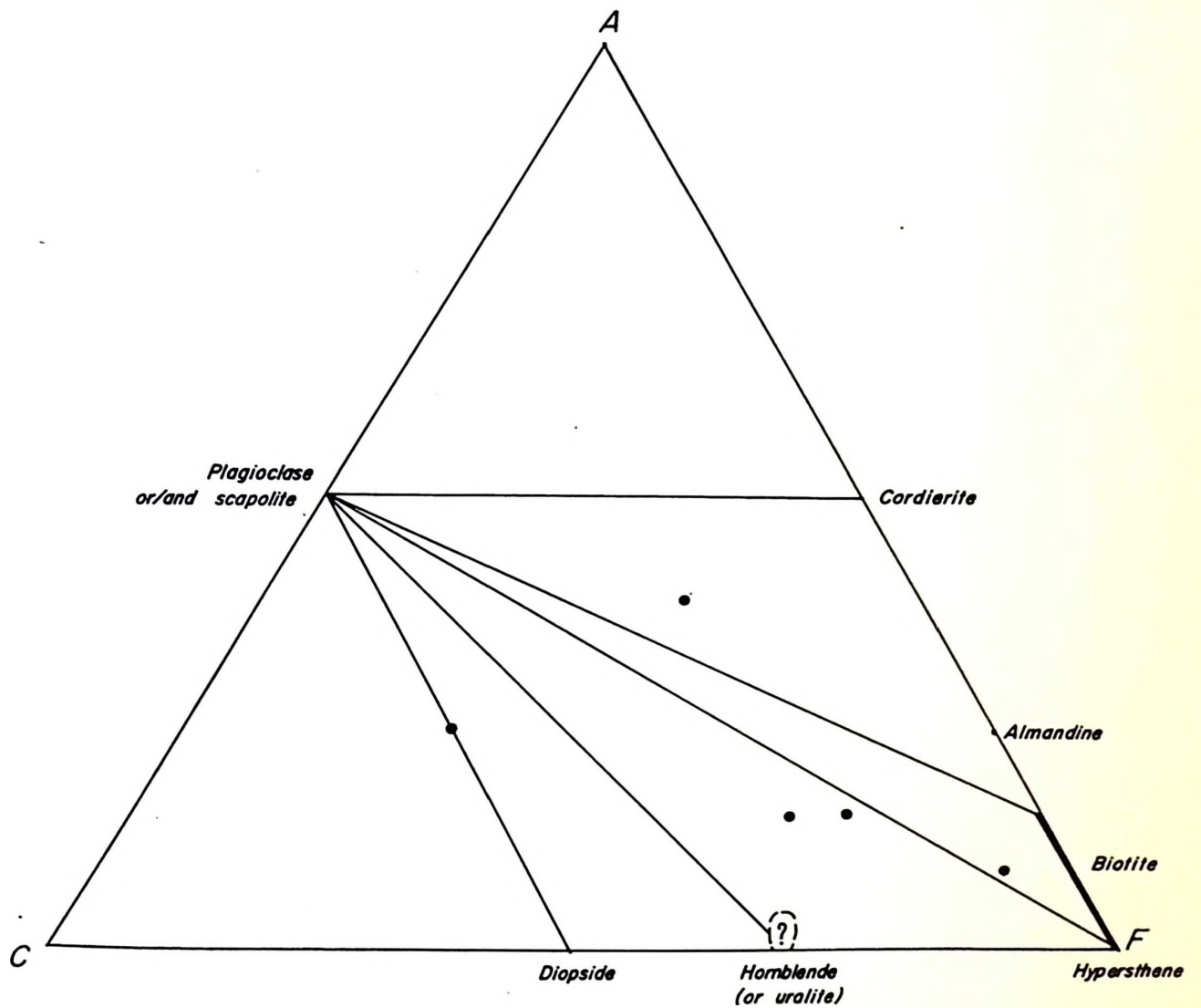


Fig. 4 ACF diagram of the pyroxene hornfels facies. (Modified from Fyfe, Turner and Verhoogen, 1958, Fig. 91)

amount of hornblende present. Eskola recognized that the hornblende hornfels facies formed at lower temperature and higher pressure than the pyroxene hornfels facies. The presence of hornblende in the pyroxene hornfels facies may be attributed either to an increase of  $P_{H_2O}$  when the temperature decreased, leading to alteration of hypersthene to urialite as a kind of retrograde metamorphic product, or the hornblende was formed by regional metamorphism, and during contact metamorphism,  $P_{H_2O}$  was high enough to maintain the stability of hornblende above the temperature limit.

The temperature of the contact metamorphism is uncertain, since  $P_{H_2O}$  and  $P_{CO_2}$  can change considerably the mineral stability fields. Turner (1948) considered  $700^{\circ}$ - $750^{\circ}$ C is not too low a value to place upon the temperature of transition between the pyroxene hornfels and the amphibolite facies. Shaw (1962) suggested that the contact metamorphism took place at a temperature in the range of  $600^{\circ}$ - $800^{\circ}$ C at a pressure equivalent to a depth of 5-10 km, and that the earlier regional metamorphism took place at a lower temperature ( $500^{\circ}$ - $700^{\circ}$ C) and at a greater depth (15-20 km).

## ELEMENT PARTITION BETWEEN HORNBLLENDE AND BIOTITE

### Introduction

Minor element distributions in coexisting minerals of metamorphic rocks may be expected to follow the behaviour of major elements in some type of crystal structural substitution under the equilibrium conditions of each metamorphic grade, if contamination or adsorption are not major factors. The more similar the bonding behaviour of a minor element is to a given major element, the closer should be the values of the distribution coefficients of the two elements.

Bonding behaviour similarities may be related to the similarity of ionic size, charge, polarizing power, electronegativity or other factors, as considered by many authors, but it is difficult to show which of these are truly important in controlling the distribution of elements.

It is possible for a minor element to substitute a major element provided that this substitution does not weaken the stability of the structure. Major element distribution among coexisting minerals depends on the chemical composition of the parent rocks, and on the temperature and pressure of formation. The distribution of minor elements may, therefore, be also expected to change with metamorphic grade.

### Review of Previous Work

Much work has been carried out on element distributions in coexisting minerals of igneous rocks, by laboratory experiments and field occurrences. However, the process of crystal growth from liquid is quite

different from the metamorphic process of solid-solid reactions. At present it is difficult to find critical evidence to distinguish geochemical differences between these two processes. To avoid confusion, the following brief review concerns the distribution of elements in coexisting minerals of metamorphic rocks only.

Nickel (1954), using a spectrographic method, analyzed major and minor constituents of coexisting chlorite, biotite and hornblende from a schist body in the Michipicoten District of Ontario. His interpretation of the amount of elements in these minerals was made in terms of electronegativities of the major and minor elements involved. The elements with similar electronegativities behave in similar fashion. Ni, Co, Cr, Ti and V are iron-like, Mn, Zr, and Sc are more similar to magnesium.

DeVore (1955a & b) examined literature data and concluded that trace element distribution and fractionation depend upon adsorption and bond energy phenomena in relation to the major element composition of the host mineral. According to his data, the behaviour of most trace elements is exactly opposite to the fractionation predicted by bond energy considerations. Therefore, he suggested that such elements do not occupy regular lattice sites but occur on growth surfaces, imperfections, dislocations, and various interfaces within the crystal, and that the mechanism of adsorption is responsible for the fixation of the trace elements during crystal growth. However, his interpretation of trace element distribution comes from igneous samples and is therefore on the basis of liquid-solid reaction.

Experimental studies have been made by Bethke et al (1958), and by Bethke and Barton (1959), of the distribution of selenium and cadmium between sphalerite and galena, and of selenium between chalcopyrite (experimentally,  $\text{CuFeS}_{1.9}$ ) and galena. The distribution coefficients were calculated by  $K_{o(P,T)} = (\text{atomic per cent element in mineral A}) / (\text{atomic per cent element in mineral B})$  and are mainly dependent on temperature, but the nature of the dependence was not given. For the distribution of Se between chalcopyrite and galena, the effect of pressure calculated from the room temperature unit cell dimensions is small and is given by the equation,  $\log_{10} K = 1.308 - 0.0000194 P$  (in bars).

Kretz (1959) analyzed spectrographically a number of coexisting phases, including 23 biotite, 23 garnet and 16 hornblende in gneisses of the amphibolite facies from south-western Quebec. Fe, Mg, Mn, V, Ti, Ca, Na, K, Ba, Cr, Zr, Y and Sc were determined, the distribution of each element between two minerals being examined by the use of distribution diagrams (Roozboom diagram). His work was mainly directed toward the major constituents Ca, Fe and Mg, and to Ti and Mn, for which most of the Roozboom diagrams show linear relations. The distribution of V between biotite and hornblende plotted on the diagram also shows the best linear relation, but the plots of Sc, Y, Ba, Sr and Cr are quite scattered. He concluded that the regular distributions may have one of the following forms (op. cit., p. 371):

1. the distribution coefficient can be expressed by a simple ratio. For example:  $(\text{Mn}/\text{Fe}+\text{Mg}+\text{Mn in garnet})/(\text{Mn}/\text{Fe}+\text{Mg}+\text{Mn in biotite}) = \text{constant}$ . Distributions of this kind are in agreement with Nernst's distribution law.

2. the distribution of an element between two minerals is dependent on the concentration of another element in one of the minerals. For example:  $(V_2O_3 \text{ in garnet}) / (V_2O_3 \text{ in biotite}) = f(\text{Ca/Fe+Mg+Mn+Ca in garnet})$ .
3. the distribution is expressed by a curved line on the distribution diagram. For example:  $(\text{Mn/Fe+Mg+Mn in garnet})$  plotted against  $(\text{Mn/Fe+Mg+Mn+Ti in hornblende})$  defines a curved line intersecting the origin.

In another paper, Kretz (1960) presented the result of the study of Al, Fe, Mg, Mn, Ti, Ca, Na, K, Ba, V, Cr, Zr, Y and Sc in all Ca-pyroxenes, 10 Ca-amphiboles and 11 biotites in 12 skarn specimens from the same region. The plotted data show linear relationships for the major constituents Fe, Mg, Mn, and Ti, but the others are rather scattered. However, Kretz concludes that each specimen (gneisses and skarns) closely approached a state of chemical equilibrium.

For most authors, "equilibrium" is a vital factor in element partition between coexisting minerals. Kretz (1959 and 1960) suggested that the regular distributions of major elements and a few trace elements indicated that the minerals of some hand-specimens have approached chemical equilibrium, but that the scattered distribution of some elements (Cr, Zr, Y and Sc) is possibly a non-equilibrium behaviour. These two conclusions appear contradictory and are difficult to accept.

Muller (1960 & 1961) analyzed spectrographically the concentrations of Mg, Fe and Mn among coexisting actinolite, cummingtonite, Ca-pyroxene and orthopyroxene in schists from Quebec. He concluded that these rocks closely approached chemical equilibrium during metamorphism,

his criterion being the orderly distribution of Mg, Fe and Mn among co-existing actinolite, Ca-pyroxene and cummingtonite. He interpreted the distributions of elements among coexisting minerals in terms of ideal solid solution.

Turekian and Phinney (1962) studied the distribution of Ni, Co, Cr, Cu and Ba between biotite-garnet pairs in the rocks from a regional metamorphic terrain in Nova Scotia, and reached the conclusion that "Rarely in samples of hand-specimen size are equilibrium distributions of trace elements between coexisting phases observed in metamorphic sequence" (p. 1439), by virtue of the considerable scatter of the data. Later, Phinney (1963) maintained the same argument after further study of the Nova Scotia rocks. He argued that the evidence is more in favour of a lack of diffusion equilibrium, in that the Fe/Mg ratio varies among biotites little more than a centimeter apart. DeVore's contention (1955 a & b) that trace elements occur in minerals by a kind of adsorption would also necessitate that chemical equilibrium is not approached for trace elements.

Very recently, Moxham (1965) presented the distributions of 7 major elements and 17 minor elements in 20 pairs of coexisting hornblende and biotite in gneisses of the lower epidote amphibolite facies from northern Ontario. He showed that some elements, Cu, Y, Ni, Co, Sc, Cr, and Ba have linear distribution and that equilibrium is approached for these elements, but that the other elements studied do not show equilibrium distribution.

### Analytical Methods

More than one hundred samples containing hornblende and biotite were collected in the summer of 1964. About 70 thin sections were made and examined; among them, only 35 samples were chosen for further work, the rest were discarded due to:

1. Inhomogeneity of mineralogical composition found under the microscope.
2. Grain size smaller than 100 mesh ( $< 0.15$  mm).
3. Abundant inclusions such as sphene, magnetite, plagioclase or quartz in hornblende or biotite.
4. Hornblende being an alteration product.

Two of the 35 samples are diorite and syenite from Methuen township. The rest, 14 from hornblende hornfels facies and 19 from the almandine amphibolite facies as shown on the geological map, are distributed near to, or within, the contact metamorphic aureole of Loon Lake pluton, Chandos township, Ontario.

Before crushing, samples were cut as small as possible, usually less than one inch thick,  $1\frac{1}{2}$ " length and  $1\frac{1}{4}$ " width. After being crushed and pulverized, the samples were screened between 150-200 mesh and distilled water used to wash out the dust attached to the surface of the grains.

A hand magnet was used to take off magnetite or other iron oxide in the samples, before using the Frantz Isodynamic separator to isolate hornblende and biotite from other phases. After that, the sample still contained some garnet and epidote, and less quartz, feldspars or calcite. Tetrabromoethane was used to float off quartz, feldspars or calcite, and methylene iodide diluted with a very small amount of acetone to separate

hornblende and biotite. Methylene iodide was then mixed with a carefully controlled amount of acetone to separate biotite from hornblende. The separation procedures were repeated several times, until less than one foreign grain in a hundred was observed under the microscope.

All of the 35 pairs of hornblende and biotite were taken for spectrographic analyses, and wet chemical analyses were made on 8 pairs. The analyzed samples are listed in Appendix I.

Preparation of samples for spectrographic work followed the method developed by G.E. Pattenden and used in the Department of Geology, McMaster University. 50% of each sample was mixed with 50% buffer which contains 50%  $\text{Cs}_2\text{CO}_3$ , 0.125%  $\text{In}_2\text{O}_3$ , 0.025%  $\text{PdCl}_2$  and 49.8% graphite. Each sample was analyzed in triplicate. At least one standard spectrum was exposed on each plate to construct the working curves of the elements. The details of the spectrographic procedure are listed in Appendix 2. The analytical and standard lines, and the range of working curves can be found in Appendix 3. All working curves were tested with G-1 and W-1, the results in comparison with previous work being listed in Table 1. Coefficients of variation for each element were calculated by following D.M. Shaw's computer programme and are listed in Table 2.

TABLE 1. G-1 and W-1 Analyses

	G-1				W-1			
	A	B	C	D	A	B	C	D
Ga	25	-	18	16	18	-	16	22
Ti	1400	-	1500	2450	5100	-	6400	8550
Cr	tr	-	22	22	100	-	120	185
V	12	-	16	31	120	-	240	275
Li	26	-	24	22	12	-	12	11
Ni	-	1	1-2	-	54	-	80	78
Co	-	2.1	2.3	-	35	63-78	52	47
Cu	9.5-15	8.7-11.1	13	3.4	-	45-54	110	190
Mn	250	-	230	220	780	108-119	1320	1150
Sc	-	-	3	-	17	-	33	31
Zr	145	-	210	93	86	-	100	88
Sr	250	-	265	300	150	-	175-220	200
Ba	1150	-	1120	1250	120-170	-	225	223
Rb	-	221-254	220	210	-	26-29	22	23

A - Shaw (1960)

B - Smales (1955)

C - Fleischer and Stevens (1962) recommended values

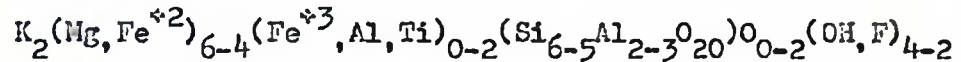
D - present work

TABLE 2. Variation coefficient of spectrographic analyses

Be	10.33%	Co	6.93%
Ga	10.46%	Cu	13.02%
Ti	17.15%	Mn	6.31%
Cr	7.61%	Zr	10.77%
V	7.86%	Sr	12.30%
Li	7.71%	Ba	8.01%
Ni	5.41%	Rb	10.96%

Mineral Composition and Calculation of Molecular Formula

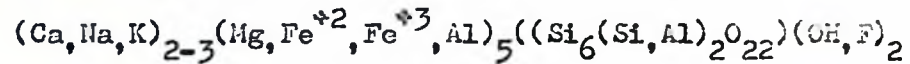
The formula of biotite can be expressed as



or



The formula of hornblende can be expressed as



or



Here X, Y and Z are as follows:

	Coordination	Radius	Major Ions	Minor Ions
X	8-12	0.90Å	K, Na, Ca	Ba, Rb, Sr, (Mn)
Y	6	.65-.90Å	Al, Mg, Fe	Mn, Cr, Ti, Li, Ni, Co, Cu, Sc, Zr, V
Z	4	.35-.60Å	Si, Al	Fe <sup>+3</sup> , (Ti), Be, Ga.

(elements in brackets are transitional and may be found in two coordinations)

To check the agreement with the theoretical formula and for calculation of distribution coefficients, the wet chemical results were recalculated into molecular formulae on the basis of 24 oxygen. The results were quite close to the theoretical formulae as shown in Appendix 4. The calculation procedures were as follows:

1.  $(\text{Weight per cent oxide}) \times (\text{number of cations in oxide}) \times 10 / \text{molecular weight of oxide}$   
= number of cations  
= A
2.  $A \times (\text{valance of cation} / \text{valance of oxygen})$   
= oxygen equivalent  
= B
3.  $A \times (24 / \Sigma B)$   
= number of cations in molecular formula  
= C

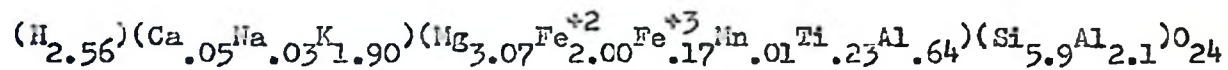
Following the above procedures, biotite sample No. 703 is taken as an example, the calculations following:

	Wt. %	A	B	(24/ΣB)	C
SiO <sub>2</sub>	38.25	$38.25 \times 10 / 60.06 = 6.369$	$x 4/2 = 12.738$	$x .9266 = 5.901$	$\rightarrow 8.000 = Z$
TiO <sub>2</sub>	1.98	$1.98 \times 10 / 79.90 = .248$	$x 4/2 = .496$	$x .9266 = .230$	↑ 2.099
Al <sub>2</sub> O <sub>3</sub>	15.04	$15.04 \times 20 / 101.94 = 2.951$	$x 3/2 = 4.427$	$x .9266 = 2.734$	
Fe <sub>2</sub> O <sub>3</sub>	1.49	$1.49 \times 20 / 159.70 = .187$	$x 3/2 = .281$	$x .9266 = .173$	↓ 6.117 = Y
FeO	15.53	$15.53 \times 10 / 71.85 = 2.161$	$x 2/2 = 2.161$	$x .9266 = 2.002$	
MnO	.08	$.08 \times 10 / 70.93 = .011$	$x 2/2 = .001$	$x .9266 = .010$	}
MgO	13.35	$13.35 \times 10 / 40.32 = 3.311$	$x 2/2 = 3.311$	$x .9266 = 3.067$	
CaO	.30	$.30 \times 10 / 56.08 = .053$	$x 2/2 = .053$	$x .9266 = .049$	} 1.979 = X
Na <sub>2</sub> O	.10	$.10 \times 20 / 62.00 = .032$	$x 1/2 = .016$	$x .9266 = .030$	
K <sub>2</sub> O	9.66	$9.66 \times 20 / 94.19 = 2.051$	$x 1/2 = 1.026$	$x .9266 = 1.900$	}
H <sub>2</sub> O	2.49	$2.49 \times 20 / 18.02 = 2.764$	$x 1/2 = 1.382$	$x .9266 = 2.561$	
sum	98.34*		25.902		

$$(24/\Sigma B = 24/25.902 = 0.9266$$

\* Deficiency probably fluorine

Therefore, the molecular formula is:



The method for hornblende is similar to the above. The results seem satisfactory in comparison with the theoretical molecular formula.

## MAJOR ELEMENT DISTRIBUTION BETWEEN HORNBLENDE AND BIOTITE

Distribution of major elements between coexisting hornblende and biotite has been considered by several authors. Most of these neglected the importance of mineral structure and site coordination, and in consequence, were unable to show realistically the relations between minor and major elements. Kretz (1959, 1960 and 1961) interpreted the distribution of octahedrally coordinated major elements using the total number of atoms of Fe, Mg, Mn and Ti as a group, and the proportion of octahedral Al was ignored. Moxham (1965) similarly proceeded under the assumption that all Al atoms are tetrahedrally coordinated. The mineral analyses discussed in the last section showed that Al atoms occupy 25-30% of the tetrahedral sites, and 6-10% of the octahedral sites of biotite, and 18-20% of the tetrahedral sites and 7-12% of the octahedral sites of hornblende.

If we consider two phases,  $\alpha$  and  $\beta$ , containing  $C$  components, the affinity of transfer of component  $i$  from one phase to the other is

$$A = \mu_i^\alpha - \mu_i^\beta \quad (\text{Prigogine and Defay, 1954, equation 6.73})$$

and

$$\mu_i^\alpha = \mu_i^{\text{Ox}}(T, p) + RT \ln x_i^\alpha \gamma_i^\alpha$$

$$\mu_i^\beta = \mu_i^{\text{Ox}}(T, p) + RT \ln x_i^\beta \gamma_i^\beta$$

where  $\mu_i^\alpha$ ,  $x_i^\alpha$  and  $\gamma_i^\alpha$  denote the potential, the molar fraction and the activity coefficient of  $i$  in phase  $\alpha$ ;  $\mu_i^{\text{Ox}}$  denotes the potential at unit activity.

Therefore

$$\Delta = \mu_i^{\alpha} - \mu_i^{\beta} + RT \ln \frac{x_i^{\alpha} \gamma_i^{\alpha}}{x_i^{\beta} \gamma_i^{\beta}} \quad (1)$$

Let 
$$\mu_i^{\alpha} - \mu_i^{\beta} = RT \ln K_i (T, p) \quad (2)$$

then (1) becomes

$$\Delta = RT \ln K_i (T, p) + RT \ln \frac{x_i^{\alpha} \gamma_i^{\alpha}}{x_i^{\beta} \gamma_i^{\beta}} \quad (3)$$

At equilibrium

$$\Delta = 0$$

and, we obtain the general form of the Nernst distribution law:

$$\frac{x_i^{\alpha} \gamma_i^{\alpha}}{x_i^{\beta} \gamma_i^{\beta}} = K_i (T, p) \quad (\text{idem. equation 18.13}) \quad (4)$$

Equation (4) denotes the equilibrium distribution of component 1 between one phase and another in a heterogeneous system, but the activity coefficients,  $\gamma_i^{\alpha}$  and  $\gamma_i^{\beta}$ , are unknown at present. If we assume that the two phases are ideal mixtures, so that

$$\gamma_i^{\alpha} = \gamma_i^{\beta} = 1,$$

then

$$x_i^{\alpha} / x_i^{\beta} = K_i (T, p) = D_i \quad (5)$$

Equation (5) is Nernst distribution law, in which the equilibrium constant,  $K_i$ , depends solely upon the temperature and pressure, and is independent of the composition of the system.  $D_i$  defines the distribution coefficient of  $i$ .

Alternatively, according to Kretz (1961, equation (4)), if two elements A and B can substitute for each other at an equivalent site in two phases  $\alpha$  and  $\beta$  in equilibrium at a given temperature and pressure, the "distribution coefficient" - as called by Kretz, with reference to species A is given by:

$$\frac{x_A^\alpha (1 - x_A^\beta)}{(1 - x_A^\alpha) x_A^\beta} = \frac{f_B^\alpha f_A^\beta}{f_A^\alpha f_B^\beta} \cdot \frac{\lambda_B^{BM} \lambda_A^{AN}}{\lambda_A^{AM} \lambda_B^{BN}}$$

If  $n_A^\alpha$  denotes the number of moles of A in  $\alpha$ , then  $x_A^\alpha = n_A^\alpha / (n_A^\alpha + n_B^\alpha)$ ,  $f$  denotes activity coefficient and  $\lambda$  denotes absolute activity (Kretz, 1961, p. 361). If ideal solutions are again assumed, so that  $f = 1$  in every case, the right hand side is constant and may be written  $K_A$ : this will be referred to as "Kretz ratio" since that author was not consistent in his usage of the term "distribution coefficient".

Thus

$$\frac{x_A^\alpha (1 - x_A^\beta)}{(1 - x_A^\alpha) x_A^\beta} = K_A \quad (6)$$

This may be written in the equivalent form

$$K_A = \frac{x_A^\alpha}{x_B^\alpha} \cdot \frac{x_B^\beta}{x_A^\beta} \quad (7)$$

or  $K_A = D_A / D_B \quad (8)$

and  $K_A = 1 / K_B \quad (9)$

According to Nernst distribution law, both  $X_A^\alpha/X_A^\beta$  and  $X_B^\alpha/X_B^\beta$  in equation (7) are equilibrium constants, and  $X_A^\alpha$  plotted against  $X_A^\beta$  or  $X_B^\alpha$  against  $X_B^\beta$  will be a straight line. However, Kretz (1961) stated that "if  $X_A^\alpha$  is plotted against  $X_A^\beta$  for a number of phase pairs, the points so produced define a curve" (p. 367) and not a straight line. Therefore, according to Kretz, the distribution of one component between two phases in ideal mixtures is not only dependent on temperature and pressure, but also depends on the composition of the system. That is, Nernst distribution law is not obeyed.

Also, Kretz (1961) concluded that for coexisting phases  $\alpha = (A,B,C)M$  and  $\beta = (A,B,C)N$ .  $K_A$  as defined by equation (6) depends on the ratio B/C in each phase. Again, Nernst distribution law is not obeyed. Kretz' reasoning is faulty and  $K_A$  has no clear meaning in this case, however its value will be examined shortly.

The tetrahedral cations have been assumed to be Si and  $Al^{(4)}$ , so

$$X_{Si} = 1 - X_{Al^{(4)}}$$

and equation (6) should apply. It is unnecessary to compute  $K(Al^{(4)})$ , since this is the reciprocal of  $K(Si)$  as shown in equation (9).

Octahedral cations include Mg,  $Fe^{+2}$ ,  $Fe^{+3}$ ,  $Al^{(6)}$ ,  $Ti^{+4}$  and  $Mn^{+4}$ , of which the latter two elements are minor and may for the present be ignored, so that

$$X_{Mg} = 1 - X_{Fe^{+2}} - X_{Fe^{+3}} - X_{Al^{(6)}}$$

Equation (6) thus reduces to

$$\frac{x_{Hg}^{Hb}}{x_{Fe^{+2}}^{Hb} + x_{Fe^{+3}}^{Hb} + x_{Al(6)}^{Hb}} \cdot \frac{x_{Fe^{+2}}^{Bio} + x_{Fe^{+3}}^{Bio} + x_{Al(6)}^{Bio}}{x_{Mg}^{Bio}} = K_{Hg}$$

Cations in 8- or 12-fold coordination include Ca, Na and K, so by a similar argument

$$K_{Ca} = \frac{x_{Ca}^{Hb}}{x_{Ca}^{Bio}} \cdot \frac{x_{Na}^{Bio} + x_{K}^{Bio}}{x_{Na}^{Hb} + x_{K}^{Hb}}$$

Nernst distribution coefficient  $D$  and Kretz ratio  $K$  were calculated according to the coordination number of elements in the analyzed minerals and are presented in Table 3.

In Table 3, one can find that the values of either  $D$  or  $K$  of any element (except Na and Ca) are very constant, but still have some deviation. If the deviation may be attributed to temperature variation (since the pressure effect is small), and if  $T_2$  is higher than  $T_1$ , then according to Kretz (1961) equation (37):

$$K_2/K_1 = \exp (\Delta H/R) (1/T_1 - 1/T_2) > 1$$

therefore

$$K_2 > K_1$$

In a two-component system, by equation (9), if  $K(A)_2 > K(A)_1$ , then one can expect that  $K(B)_1 > K(B)_2$ .

It is believed that the rock closer to the intrusive body had the higher temperature of metamorphism, so comparing sample numbers as shown in geological map,  $T_{(703)} > T_{(733)} > T_{(704)}$  and  $T_{(724)} > T_{(744)} > T_{(753)} > T_{(761)}$ . However, values of D or K as listed in Table 4 are not in agreement with these assumed temperature variations, that is, there is no accordance of the D or K values changing with the temperature. The water content in syenitic and granitic magma is uncertain and most of the rocks in this study usually contain some calcium carbonate, so that the variation of D or K may be the result of different  $P_{H_2O}$  or  $P_{CO_2}$  as well as temperature. Or perhaps, there may have been interaction of different structure sites as Kretz (1960) pointed out, since the distribution of an element is a function of the concentration of other elements in one or both of the coexisting minerals.

TABLE 3. Values of K and D

Temperature	Low → High			Low → High					
Region	Owenbrock			Lasswade					
Sample	704	788	703	761	756	755	744	724	mean
Metamorphic grade	AA*	AA	AA	AA	EE**	EE	EE	EE	
Coordination 4									
D ( Si )	1.10	1.09	1.07	1.12	1.12	1.13	1.14	1.11	1.11
D ( Al <sup>(4)</sup> )	.70	.74	.79	.69	.70	.67	.66	.69	.72
K ( Si )	1.43	1.47	1.34	1.63	1.61	1.68	1.72	1.61	1.56
Coordination 6									
D ( Mg )	.86	.85	.85	1.08	.90	.97	.87	.92	.91
D ( Σ Fe )	1.17	1.19	1.23	1.01	1.18	1.17	1.22	1.12	1.16
D ( Al <sup>(6)</sup> )	1.39	1.23	1.18	1.04	.90	.77	1.13	1.21	1.11
D ( Ti )	.35	.40	.35	.45	.60	.49	.45	.37	.43
D ( Mn )	1.90	2.00	2.06	1.73	1.73	1.98	1.61	1.83	1.86
D ( Fe <sup>+2</sup> )	.92	1.00	1.04	.91	.93	.89	.96	.89	.94
D ( Fe <sup>+3</sup> )	3.00	3.63	3.26	2.02	2.57	2.62	2.36	2.78	2.78
K ( Mg )	.79	.74	.73	1.13	.84	.94	.75	.86	.85
K ( Σ Fe )	1.33	1.34	1.40	1.01	1.31	1.27	1.39	1.23	1.29
K ( Al <sup>(6)</sup> )	1.44	1.26	1.20	1.40	.89	.76	1.13	1.23	1.12
Coordination 8 to 12									
D ( K )	.14	.14	.16	.12	.12	.09	.11	.11	.12
D ( Na )	9.15	8.37	6.58	9.33	10.50	4.38	7.03	9.97	7.91
D ( Ca )	20.2	15.8	30.1	18.2	16.7	11.4	10.5	14.6	
K ( K )	.0082	.0102	.0076	.0079	.0076	.0103	.0115	.0084	.0090
K ( Na )	10.48	9.65	7.20	10.93	12.11	4.97	8.22	9.32	9.11
K ( Ca )	71.8	54.0	115.6	63.1	62.7	45.9	36.8	53.2	

\* Almandine amphibolite facies

\*\* Hornblende hornfels facies

### MINOR ELEMENT PARTITION BETWEEN HORNBLLENDE AND BIOTITE

Minor elements in hornblende and biotite can be considered as following the behaviour of major elements, if contaminated samples are avoided and if "adsorption" (DeVore, 1955a) is not an important factor.

Nernst distribution law (equation (5)) is believed to be applicable to the distribution of a minor element, T, between hornblende and biotite. From Table 3, it can be seen that the value of D for a major element, M, is approximately constant. The relation between D(T) and D(M) may thus be written,

$$D(T) = C \times D(M) \quad (10)$$

where C is expected to be constant (at a given T and P)

If a minor element, T, behaves the same way as a given major element, M, in both hornblende and biotite, then

$$N_T^{\text{Hb}} / N_T^{\text{Bio}} = N_M^{\text{Hb}} / N_M^{\text{Bio}} \quad (11)$$

where  $N_T^{\text{Hb}}$  is the number of T atoms in hornblende and similarly for the other symbols. Since  $X_T^{\text{Hb}} = N_T^{\text{Hb}} / (\text{Total atoms in similar coordinated position})$ , therefore, equation (11) becomes

$$X_T^{\text{Hb}} / X_T^{\text{Bio}} = X_M^{\text{Hb}} / X_M^{\text{Bio}}$$

or  $D(T) = D(M) \quad (12)$

Equation (12) shows that when a minor element behaves the same way as a given major element, the distribution coefficients of both elements will be the same. In comparing with equation (10) and (12), it can be seen that the stronger the geochemical coherence of a minor and a given major element, the closer the value of C in equation (10) to 1. This will be tested in the following discussion.

In the distribution diagrams (Figs. 5-18) which accompany the following sections, the units in every case are gram-atoms per million grams, abbreviated to "atoms".

#### Minor Elements in Tetrahedral Coordination

In order to compare with the values of D for both minor and major elements in the following discussion, the ratio of atomic fractions between hornblende and biotite is used rather than weight ratio, although they both give equivalent results for tetrahedrally coordinated atoms.

The total number of atoms of Al<sup>(4)</sup> and Si in hornblende and biotite has been treated as a constant, so that equation (5) becomes

$$D(T) = (\text{Abundance of T in Hb}) / (\text{Abundance of T in Bio}) \quad (13)$$

Average Values of D of the elements in tetrahedral coordination are listed in the following table.

Table 4. Distribution coefficients (D), ionic radii (r) and electro-negativities (e) of cations in tetrahedral coordination (values of r are taken from Ahrens (1952) and e from Pauling).

	D	r	e
Be <sup>+2</sup>	1.5	0.35A	
Ga <sup>+3</sup>	0.7	0.62	1.82
Si <sup>+4</sup>	1.11	0.42	1.90
Al <sup>+3(4)</sup>	0.72	0.51	1.5
Ti <sup>+4</sup>	?	0.68	

Beryllium is believed to be tetrahedrally coordinated. Spectrographic analyses as listed in Appendix 5 were plotted in Roozeboom diagrams. Fig. 5 shows a little scattering with  $D(\text{Be})$  values ranging from 0.95 to 2.4. The average is roughly about 1.5 and is much closer to  $D(\text{Si})$  than to  $D(\text{Al}^{(4)})$  (see Table 4), suggesting that Be substitutes more easily for Si than for Al. In conformity with this conclusion, the ionic size of silicon is a little larger than Be and smaller than that of Al.

Gallium distribution between hornblende and biotite is somewhat scattered (Fig. 6). However, the points are distributed roughly along the line  $D = 0.7$ , which is closer to  $D(\text{Al}^{(4)})$  than that of total Al ( $D(\text{Al}) = 0.76$  or  $D(\text{Al}^{(6)}) = 1.11$ ). This suggests that Ga can substitute for Al, and probably also that most of the Ga atoms are tetrahedrally coordinated. The radii of trivalent cations of Ga and Al are so close that Ga presumably follows the behaviour of Al in both minerals. Nickel's (1954) interpretation that the minor elements behave like the major element with similar electronegativity fails to explain the present data, since the electronegativity of Ga is closer to Si than to Al, consequently, Ga should follow silicon, in fact the opposite is more acceptable.

Titanium spectrographic analyses (Fig. 7) are quite scattered, although wet chemical analyses show more regular  $D$  values. This may be partly due to the poor precision of the data as shown in Tables 1 and 2, and partly due to the uncertain behaviour of Ti which can have either tetrahedral or octahedral coordination. The data offer no clear evidence to show what major element or elements are followed by Ti.

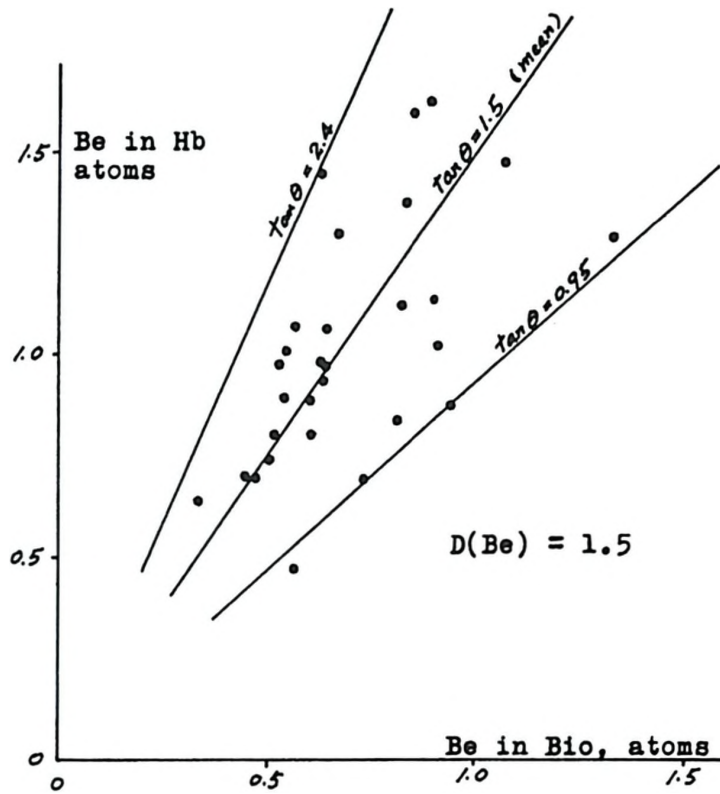


Fig. 5 Distribution of Be between hornblende and biotite

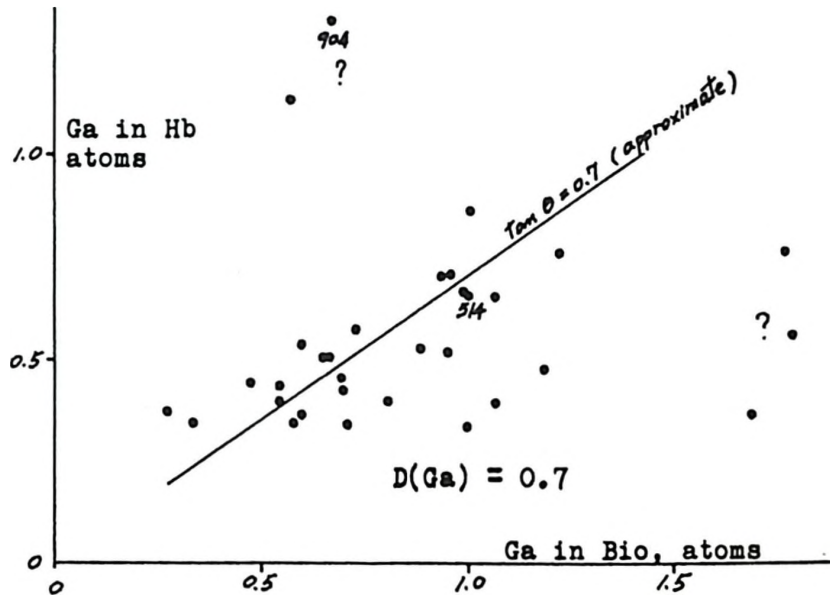


Fig. 6 Distribution of Ga between hornblende and biotite

Minor elements in Octahedral Coordination

The use of atomic fractions to calculate distribution coefficients is only possible when major element analyses of the minerals are available. For the present work, the average ratio of total number of atoms occupying octahedrally coordinated position in biotite to those in hornblende was calculated from the eight pairs of hornblende and biotite analyzed chemically to be 1.155. For mineral pairs for which major element analyses were not available, it was decided to use this average value, so that

$$D(T) = \frac{X_T^{\text{Hb}}}{X_T^{\text{Bio}}} \\ = (\text{Abundance of T in Hb} / \text{Abundance of T in Bio}) \times 1.155 \quad (14)$$

TABLE 5. Distribution coefficients (D), ionic radii (r) and electronegativities (e) of cations in octahedral coordination

	D	r	e
Cr <sup>+3</sup>	1.27	0.63 <sup>a</sup>	1.6
V <sup>+3</sup>	1.27	0.74	1.35
Li <sup>+</sup>	0.17	0.68	1.0
Ni <sup>+2</sup>	0.63	0.69	1.7
Co <sup>+2</sup>	0.63	0.72	1.7
Cu <sup>+2</sup>	?	0.72	2.0
Mn <sup>+2</sup>	2.14 <sup>*</sup> 1.85 <sup>**</sup>	0.80	1.4
Zr <sup>+4</sup>	?	0.79	1.2
Fe <sup>+3</sup>	2.78	0.64	1.8
Fe <sup>+2</sup>	0.94	0.74	1.65
ΣFe	1.16		
Mg <sup>+2</sup>	0.91	0.66	1.2
Al <sup>+3(6)</sup>	1.11	0.51	1.5

\* by spectrographic analyses

\*\* by wet chemical analyses

Chromium shows a good linear distribution (Fig. 8) with a slope of approximately 1.1, while Nickel (1955) gave 0.22 and Moxham 1.30. If corrected by equation (14),  $D(\text{Cr})$  will be 1.27 which is quite close to  $D(\text{Al}^{(6)})$  and  $D(\Sigma\text{Fe})$  (see Table 5). It seems possible that Cr can substitute for both Al and Fe in octahedrally coordinated positions, but it is not likely that Cr substitutes for Al in tetrahedral sites since  $D(\text{Al}^{(4)})$  is much lower than  $D(\text{Cr})$ . The ionic radii show that Cr substitution for these ions is quite possible, but whether it substitutes mainly for  $\text{Fe}^{+2}$  or for  $\text{Fe}^{+3}$  is uncertain. The value of  $D$  and the electronegativity for Cr are closer to those for  $\text{Fe}^{+2}$  than those for  $\text{Fe}^{+3}$ , while the radius of Cr is closer to that of  $\text{Fe}^{+3}$ .

Vanadium data are shown in Fig. 9 and are more scattered than those of Kretz (1959). The present data give  $D(\text{V}) (= 1.27)$  close to  $D(\text{Al}^{(6)})$  and  $D(\Sigma\text{Fe})$ , suggesting that the substitution of V for  $\text{Al}^{(6)}$  and Fe is possible. The common V ion in minerals is the trivalent cation, whose radius of  $0.74\text{\AA}$  is the same as that of  $\text{Fe}^{+2}$ . Whether  $\text{V}^{+3}$  more readily substitutes for  $\text{Fe}^{+2}$  than  $\text{Fe}^{+3}$  is uncertain, as in the case of Cr as shown above. The electronegativity of  $\text{Mg}^{+2}$  is the closest to that of  $\text{V}^{+3}$  than to  $\text{Al}^{+3}$ ,  $\text{Fe}^{+2}$  or  $\text{Fe}^{+3}$ , and also, the radius of  $\text{Mg}^{+2}$  is very close to that of  $\text{V}^{+3}$ . However, the present data give no suggestion that  $\text{V}^{+3}$  follows  $\text{Mg}^{+2}$ .

Lithium is present mostly in biotite as shown in Fig. 10, in which the points are distributed between the two slope lines,  $\tan \theta = 0.06$  and  $\tan \theta = 0.27$ , the average is about  $\tan \theta = 0.15$  and gives  $D(\text{Li}) = 0.17$ , which is much lower than the  $D$  value for any major

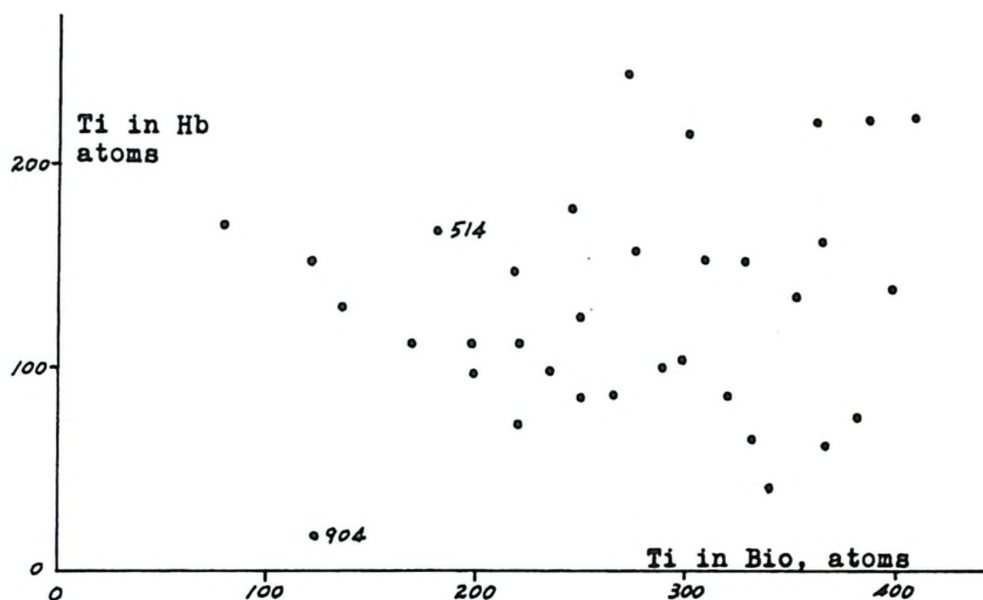


Fig. 7 Distribution of Ti between hornblende and biotite

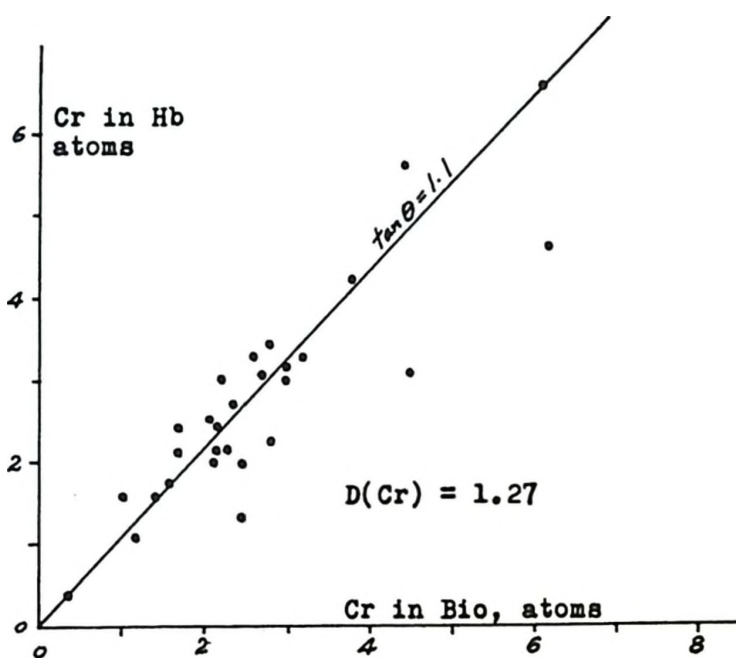


Fig. 8 Distribution of Cr between hornblende and biotite

element in octahedral coordination. Lithium can occur either in tetrahedrally coordinated site as in cryolithionite,  $\text{Na}_3\text{Al}_2(\text{LiF}_4)_3$ , or in octahedrally coordinated site as in spodumene, but the behaviour of Li in hornblende and biotite is uncertain. Although the ionic radius of Li is very close to that of other major elements in octahedral coordination, especially  $\text{Mg}^{+2}$ , the present data do not show geochemical coherence of Li with any major element. There is no data available from Kretz (1959) and Moxham (1965).

Nickel data are presented in Fig. 11, the average value of  $D(\text{Ni})$  being 0.63. Moxham's (1965) data corrected by equation (14) will give 0.81 and Nickel's (1955) 0.55. Most of the Ni in minerals is divalent and believed to be in octahedral coordination. Although  $D(\text{Ni})$  is rather lower than both  $D(\text{Mg})$  and  $D(\text{Fe}^{+2})$ , it is much lower than those of any other major elements in octahedral coordination. This probably suggests that the substitution of Ni for  $\text{Mg}^{+2}$  and  $\text{Fe}^{+2}$  is possible. The ionic radii seems to agree with this interpretation, but the electronegativities of these cations only show that the substitution of Ni for  $\text{Fe}^{+2}$  is possible.

Cobalt data show a little scatter as can be seen in Fig. 12. Most of the Co ions are in octahedral coordination. The average value of  $D(\text{Co})$  is the same as that for Ni. Moxham's data if corrected by equation (14) will give 0.86 and Nickel's 0.67. Therefore, Co probably behaves in the same fashion as Ni, that is the substitution of  $\text{Co}^{+2}$  for  $\text{Mg}^{+2}$  and  $\text{Fe}^{+2}$  is possible. The ionic radii as shown in Table 5, are in concordance with this interpretation and suggest that  $\text{Co}^{+2}$  probably prefer sites of  $\text{Fe}^{+2}$

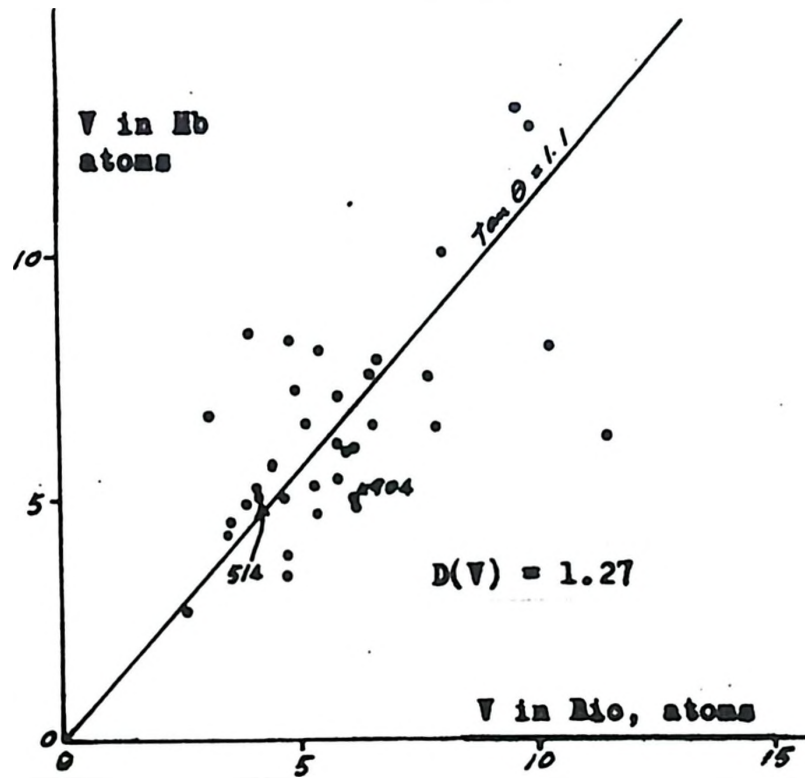


Fig. 9 Distribution of V between hornblende and biotite

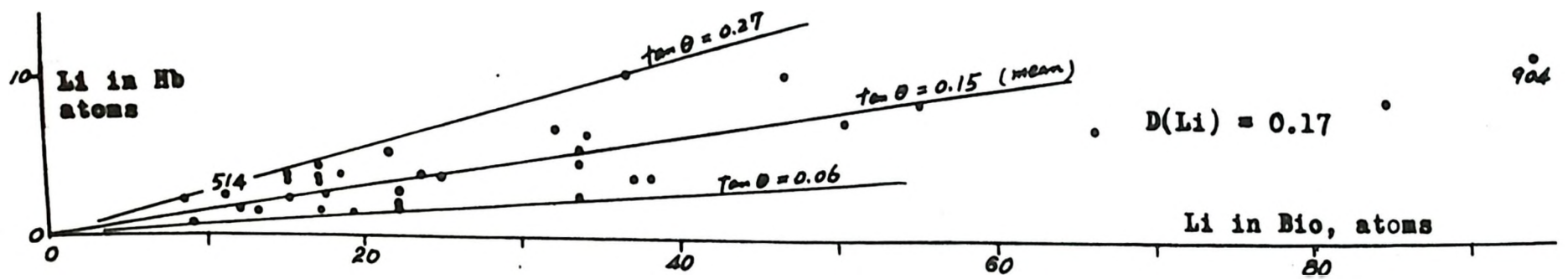


Fig. 10 Distribution of Li between hornblende and biotite

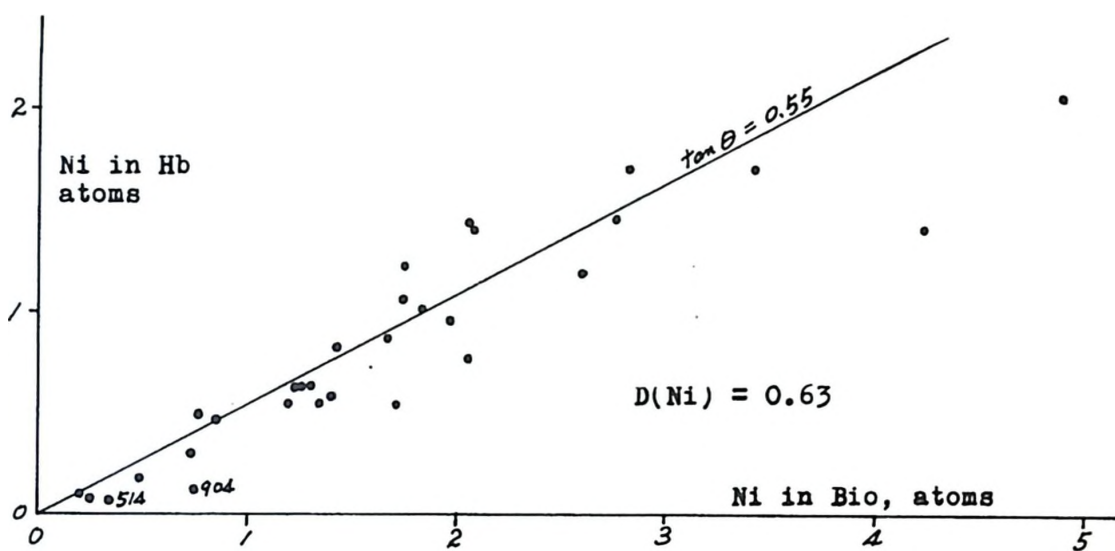


Fig. 11 Distribution of Ni between hornblende and biotite

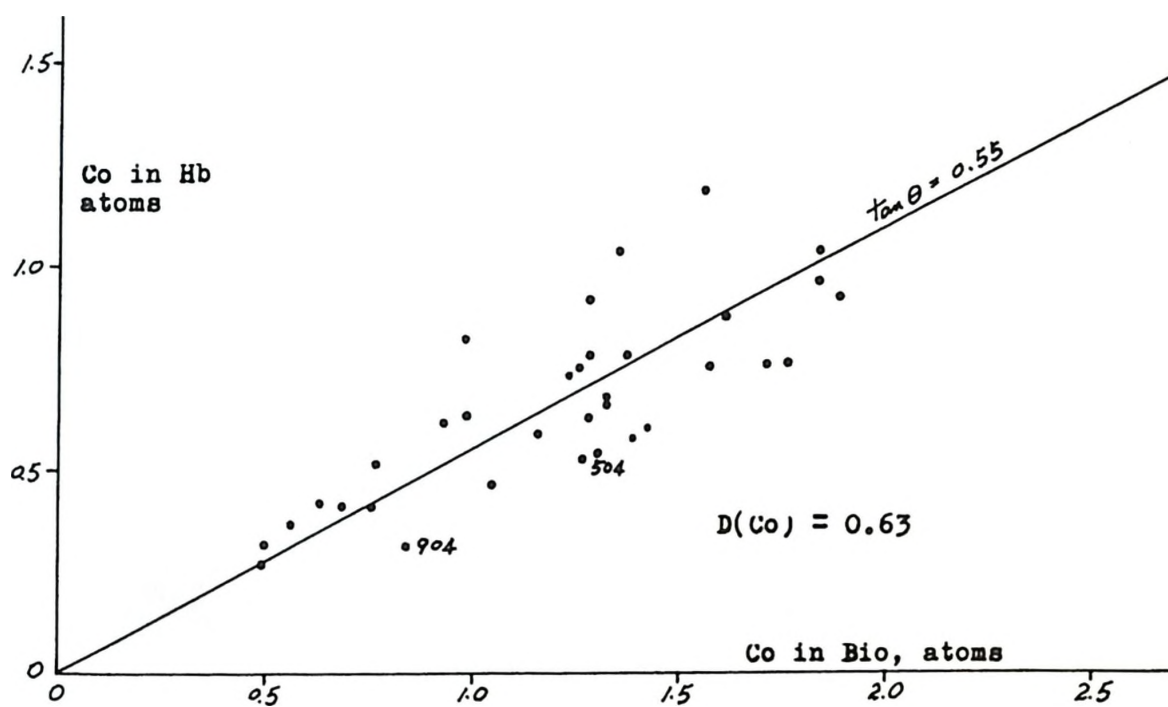


Fig. 12 Distribution of Co between hornblende and biotite

than those of  $\text{Mg}^{+2}$ . The electronegativity values give no suggestion of the possible substitution of Co for  $\text{Mg}^{+2}$ , but suggest that  $\text{Co}^{+2}$  followed  $\text{Fe}^{+2}$  is possible

Copper data is quite scattered (Fig. 13), which may be due both to the erratic substitution of Cu for major elements and the poor precision of the data as shown in Table 1 and 2. The scattered array of distribution figures of Cu also reported by both Kretz (1959) and Moxham (1965). Contamination is commonly encountered with this element and may also have played a large role.

Manganese spectrographic analyses data are plotted in Fig. 14, and give  $D(\text{Mn})$  2.14 in the average, whereas the wet chemical analyses shown in Table 5 give 1.86. Both values are lower than  $D(\text{Fe}^{+3})$  but higher than those of other major elements in octahedral coordination. Since  $\text{Mn}^{+2}$  has a larger radius than these, it may partly enter the 8- or 12-fold coordinated sites to substitute for  $\text{Ca}^{+2}$  which concentrates more in hornblende than in biotite, it may also partly distribute to octahedral positions, although the major elements to be substituted are not certain.

Zirconium data are very scattered, as shown in Fig. 15. This may be due to the analysis line of Zr  $3391\text{\AA}$  being too insensitive for the low concentration, or alternatively, the common occurrence of zircon inclusions in mafic minerals suggests that contamination has been operative. The same scattered results were reported by Kretz (1959) and Moxham (1965). Thus no explanation is suggested by the data for the behaviour of Zr distributing in hornblende and biotite.

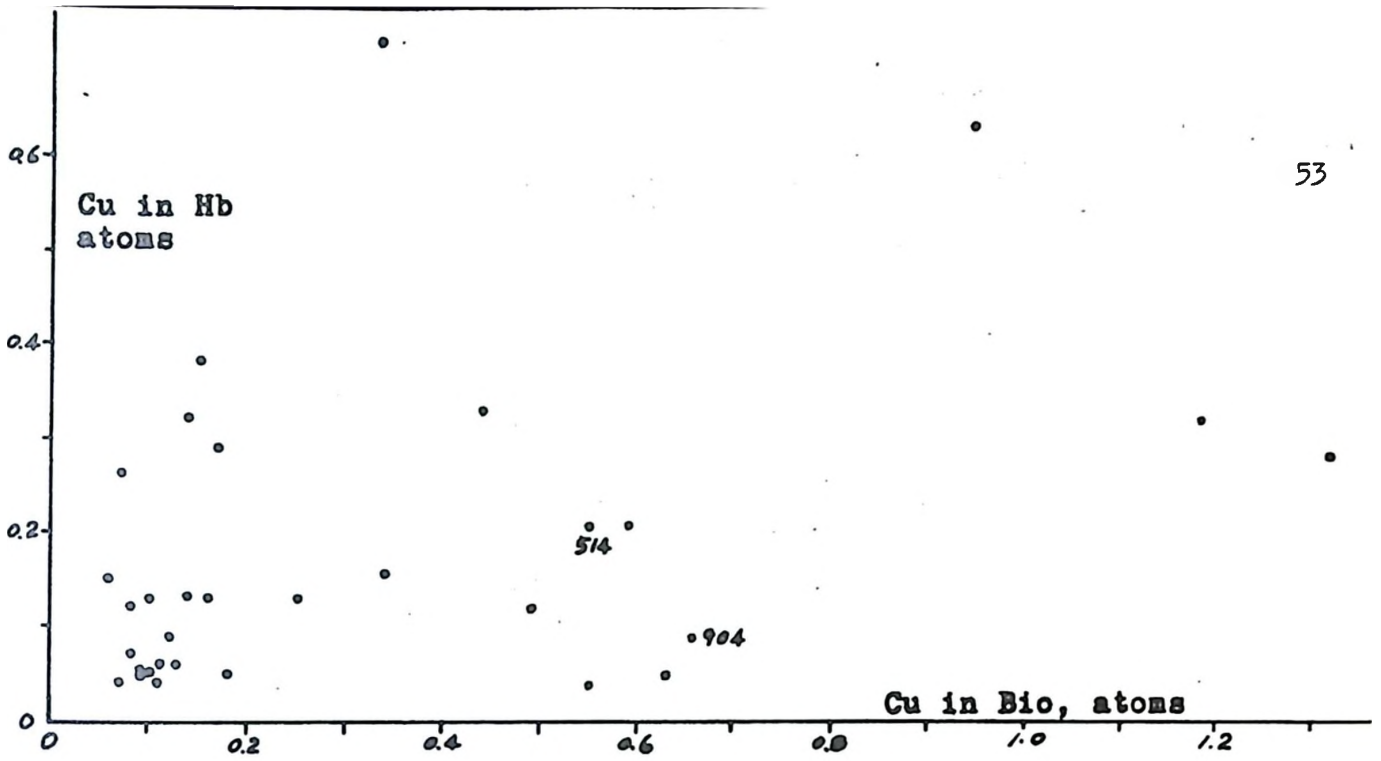


Fig. 13 Distribution of Cu between hornblende and biotite

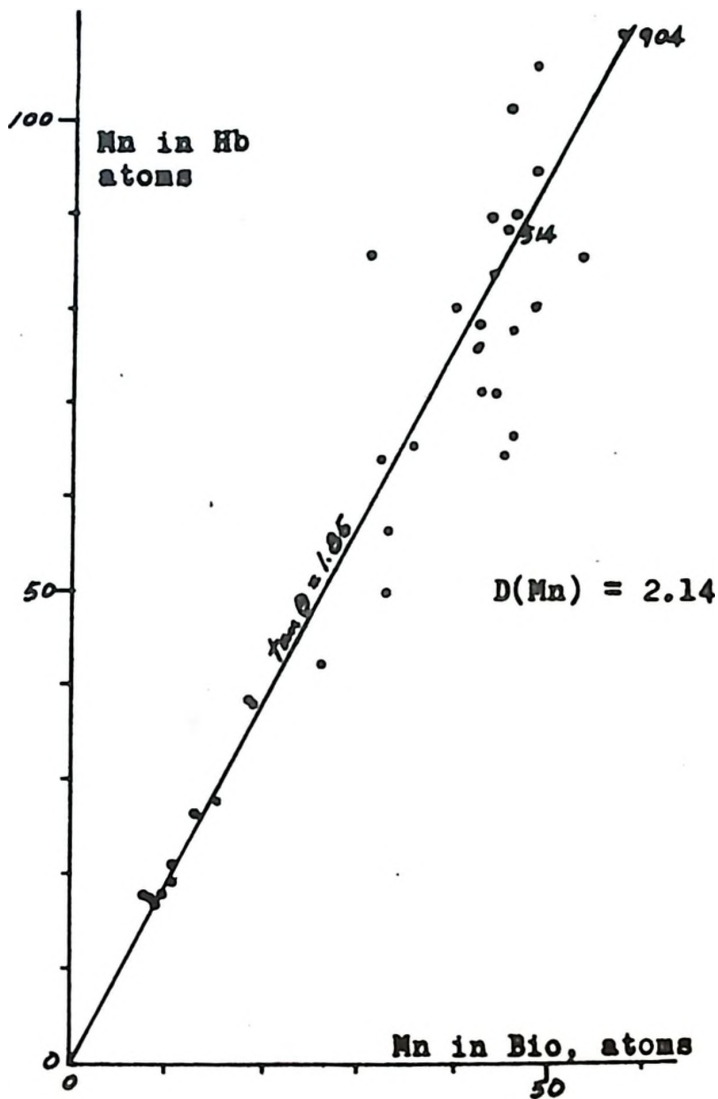


Fig. 14 Distribution of Mn between hornblende and biotite

Minor Elements in 8- or 12-Fold Coordination

It was shown above that equation (5) can be applied only when major element analyses are available for the minerals. From eight pairs of wet chemically analyzed samples, the average value of the ratio of the total number of Ca, Na, and K atoms in biotite to that in hornblende, is 0.782. Therefore, equation (5) becomes:

$$D(T) = (\text{Abundance of T in Hb} / \text{Abundance of T in Bio}) \times 0.782 \quad (15)$$

and the values of D are listed in Table 6.

TABLE 6. Distribution coefficients (D), ionic radii (r) and electronegativities (e) of cations in 8- or 12-fold coordination

	D	R	e
Sr <sup>+2</sup>	15	1.12 <sup>Å</sup>	1.0
Ba <sup>+2</sup>	0.031	1.34	0.85
Rb <sup>+</sup>	0.011	1.47	0.8
Ca <sup>+2</sup>	17.2	0.99	1.0
Na <sup>+</sup>	7.91	0.97	0.9
K <sup>+</sup>	0.12	1.33	0.8

Strontium data are plotted in Fig. 16, in which the values of D range from 2.5 to 25, with the average around 15, which is very close to D(Ca) (see Table 6), and suggests the substitution of Sr for Ca. The electronegativities and ionic radii also suggest that the substitution is possible. Moxham's (1965) data of Sr distribution between hornblende and biotite is also quite scattered, however, he agreed that Sr has a well-known geochemical coherence with Ca.

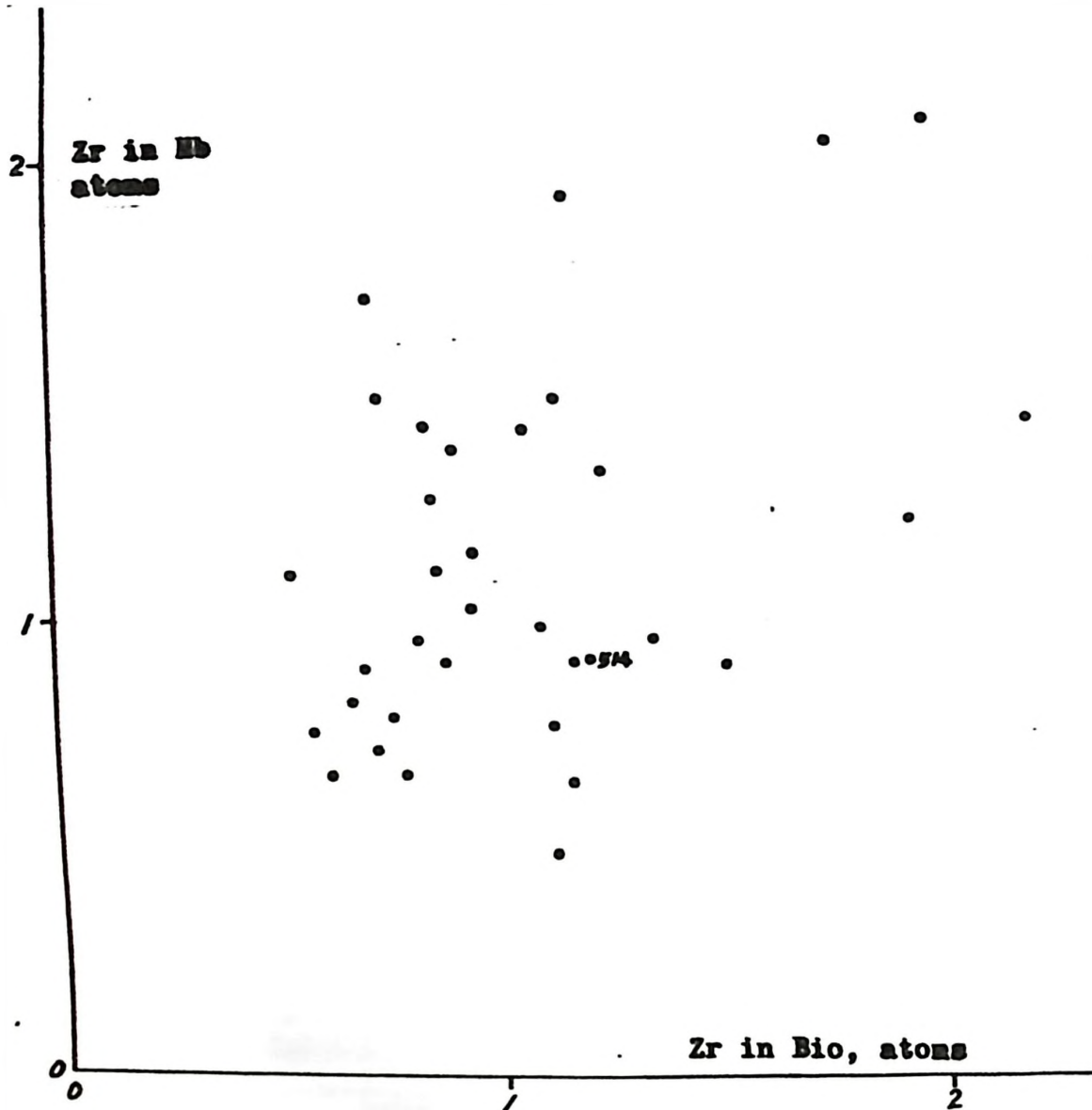


Fig. 15 Distribution of Zr between hornblende and biotite

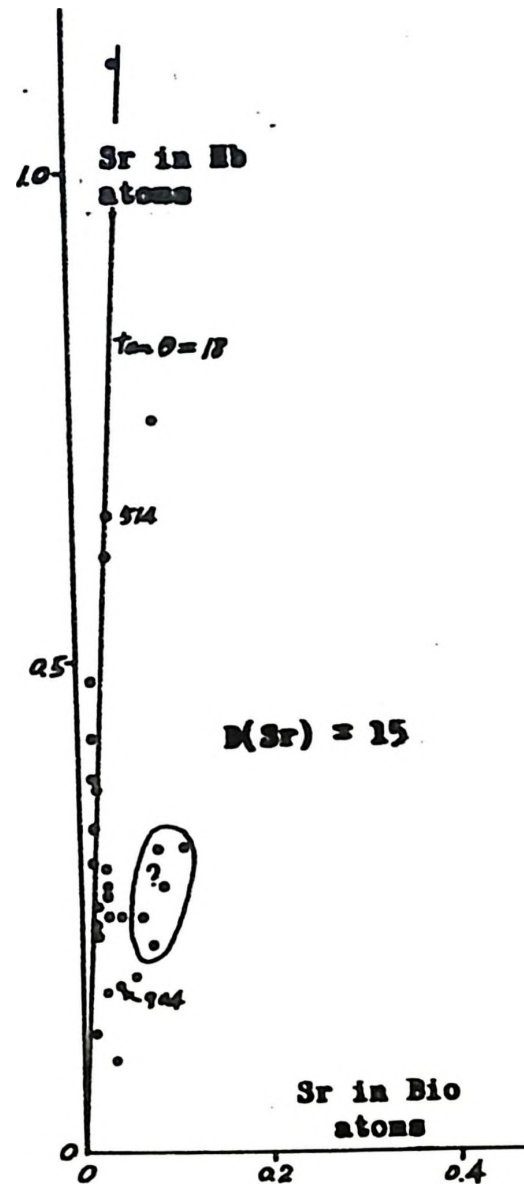


Fig. 16 Distribution of Sr between hornblende and biotite

Barium distribution data are presented in Fig. 17, which shows that Ba is strongly concentrated in biotite.  $D(\text{Ba})$  is closer to that of K than those of other major elements occupying 8- or 12-fold coordinated sites. The ionic radii and electronegativities are very similar. Therefore, it is possible that Ba can substitute for K in hornblende and biotite.

Rubidium analyses are presented in Fig. 18 and show marked scatter. The average  $D(\text{Rb})$  is 0.011 and is closer to that of  $D(\text{K})$  than to other major elements in 8- or 12-fold coordination. Also, the ionic radii and electronegativities show the similarity. Therefore, it is possible that Rb substitutes for K in hornblende and biotite. No Rb data are available from Kretz (1959) and Moxham (1965).

It is worthwhile to note that the minor element distribution between hornblende and biotite in diorite (No. 514) and in nepheline syenite (No. 904) as plotted in each figure from Fig. 5 to 18, show no significant differences from those of metamorphic rocks except for Be in both samples and Ga and Ti in No. 904. The igneous rocks were expected to have different D values but as shown above, most of the minor elements are following the major elements in the minerals, and the distribution coefficients of major elements are not changing with the temperature variations. Therefore the deviation of the distribution coefficients of minor elements can not be explained mainly by the temperature variation. This can also be seen in Fig. 19, in which values of D are not changing with metamorphic grade and the assumed temperature variation. Thus the different D values are

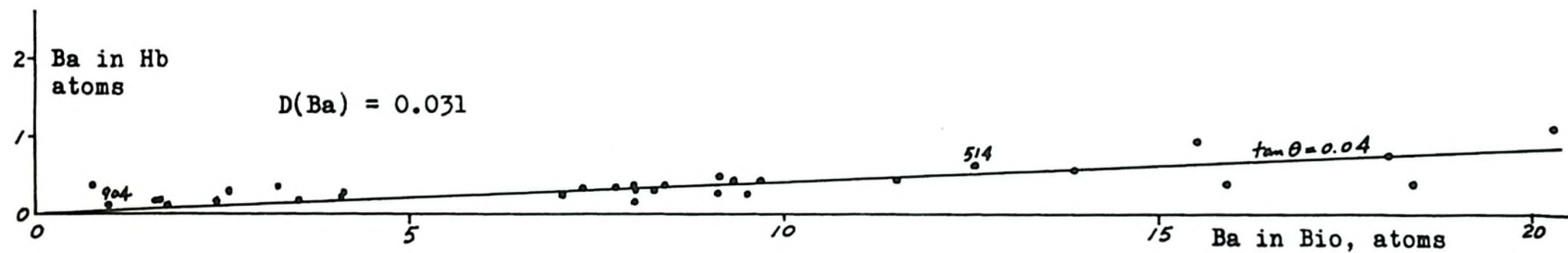


Fig. 17 Distribution of Ba between hornblende and biotite

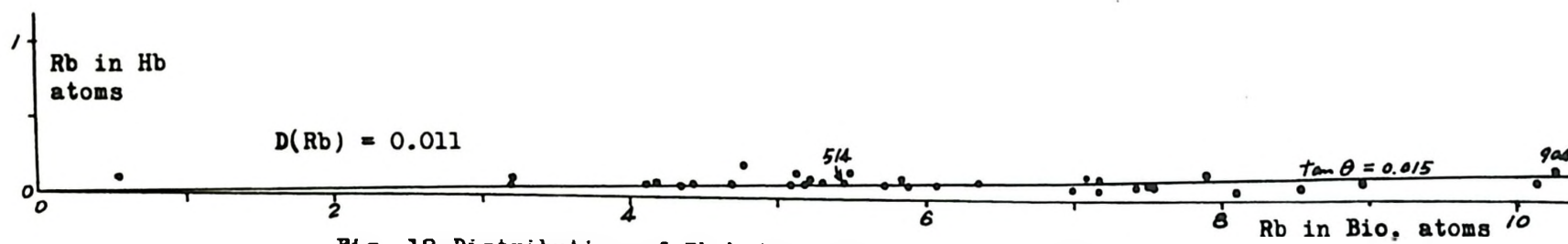


Fig. 18 Distribution of Rb between hornblende and biotite

probably due to  $P_{H_2O}$ ,  $P_{CO_2}$ , temperature, and experimental errors, and make the difference in distribution coefficients between igneous and metamorphic rocks too small to be observed.

Fig. 19 Relation of distribution coefficients (D) and metamorphic grades, abscissa roughly shows distance from syenite pluton.

Hornblende hornfels facies		Almandine amphibolite facies								
A	B	C	D	E	F	G	H	I	J	
724	604 752					747		508		Lasswade area
736	606 753					757		761		
749	607 755									
	735 756									
	739 791									
	744									
		780	781	703	710		788		704	Owenbrook area
			782	711			789		705	
			786	715						
Pluton	country rocks —— (increasing distance from syenite pluton) ——>									

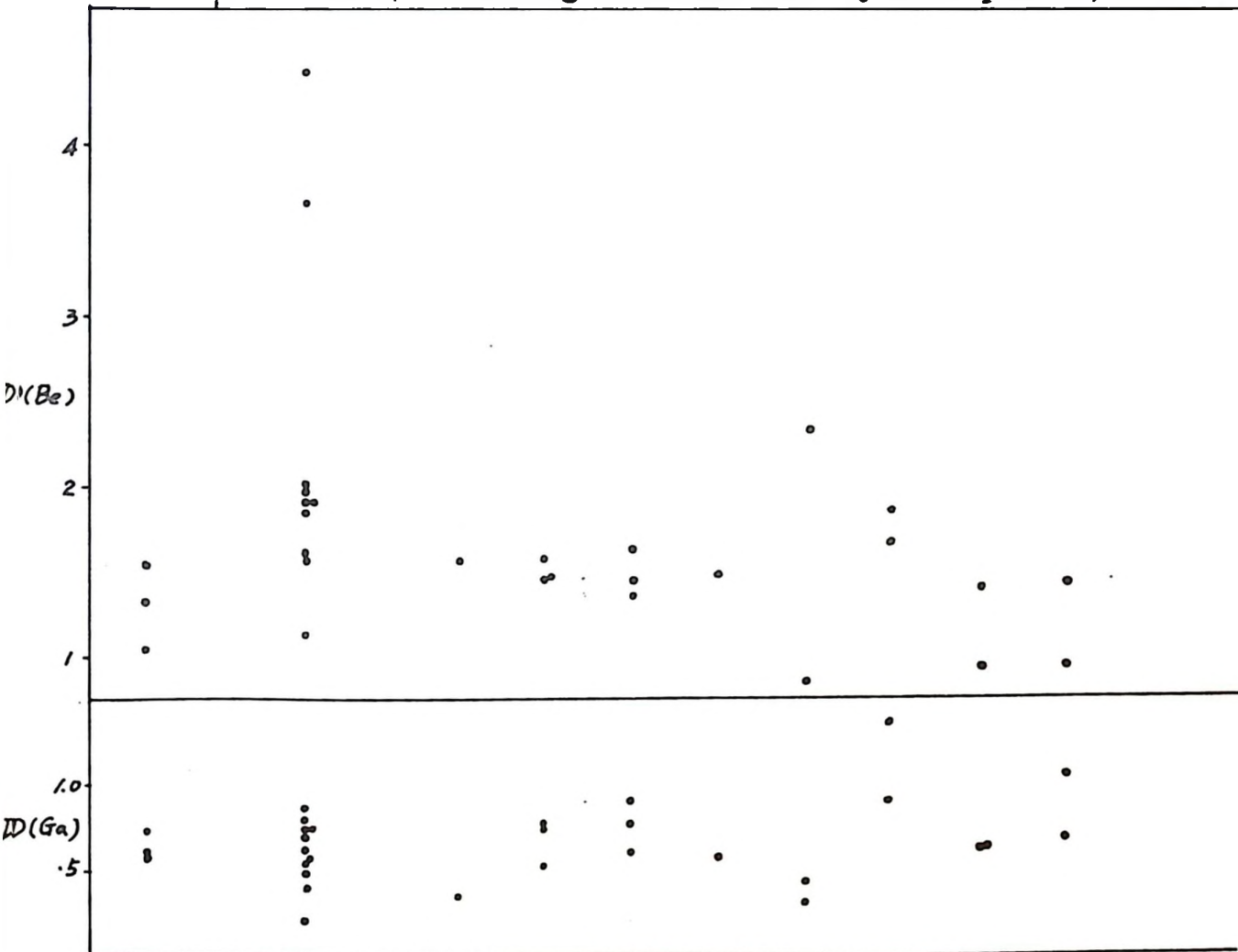


Fig. 19 (continued)

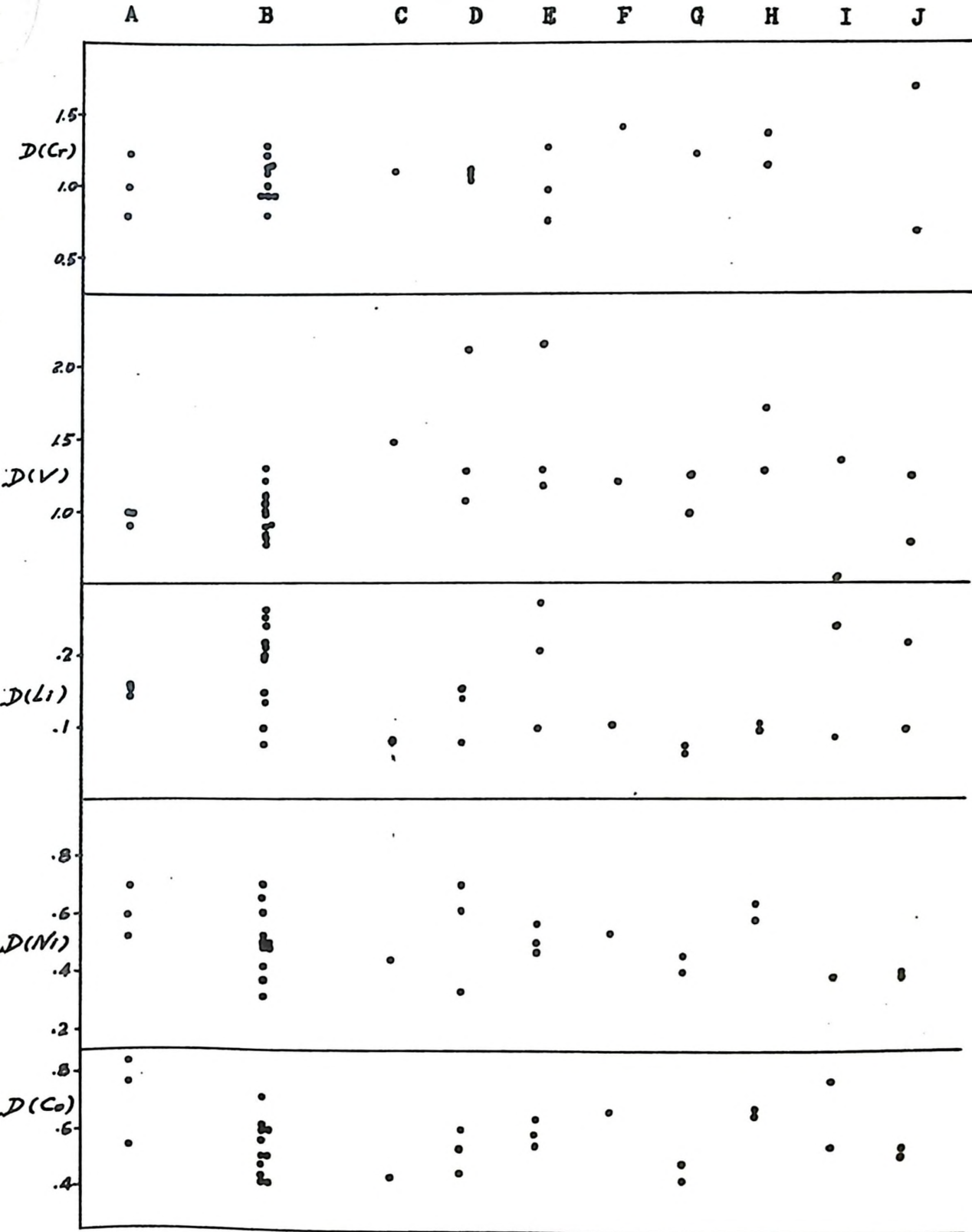
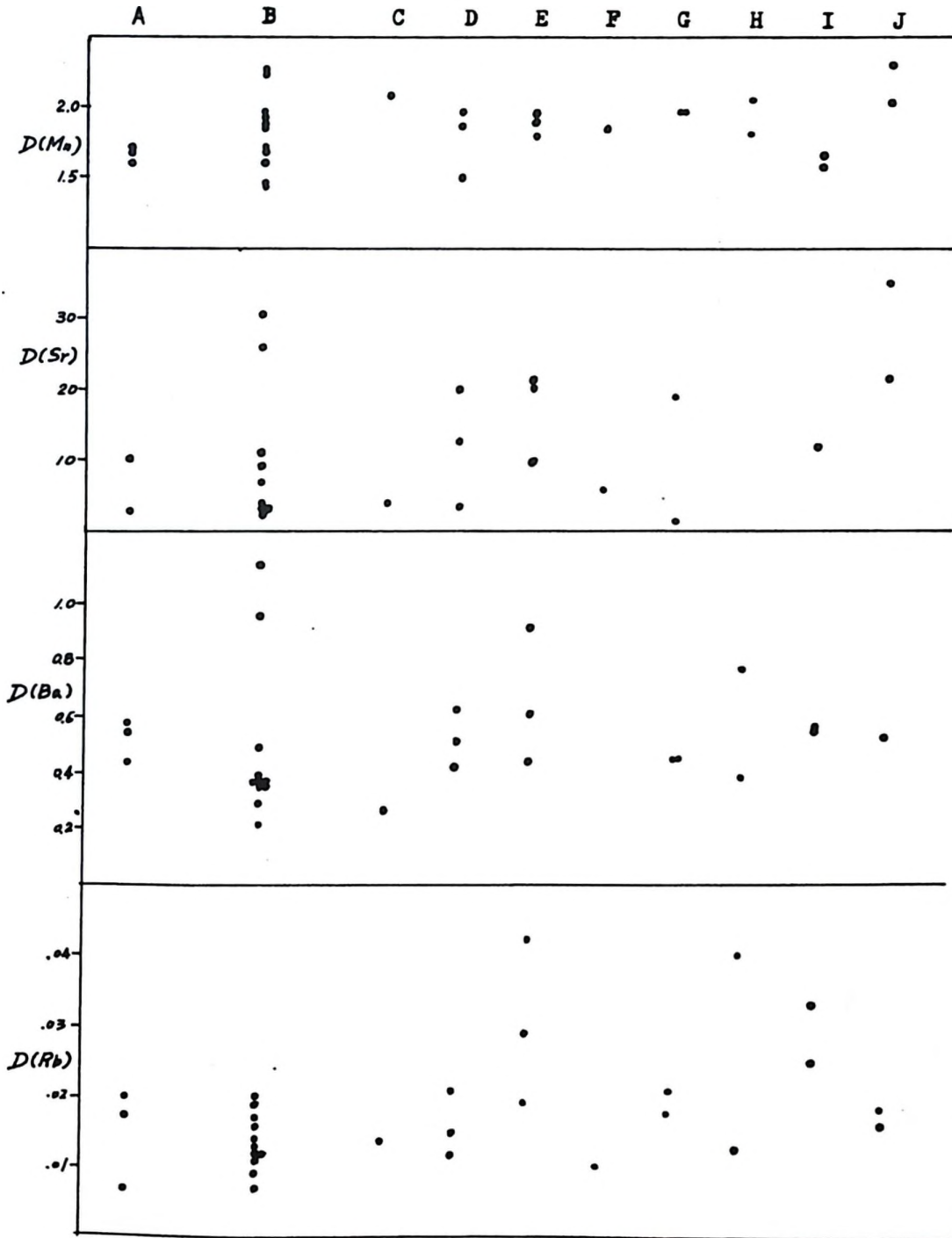


Fig. 19 (continued)



## SUMMARY

The sedimentary rocks near the Loon Lake pluton of Chandos township were metamorphosed during two periods; first, the rocks were raised to the almandine amphibolite facies by regional metamorphism. The later intrusion of the Loon Lake pluton superimposed a contact metamorphic aureole on the nearby rocks and two facies, hornblende hornfels facies and pyroxene hornfels facies, become recognizable.

It was expected that the distribution coefficients of major and minor elements between hornblende and biotite in the rocks of different metamorphic facies would show some correlation with the temperature variation of the rocks during metamorphism. However, owing to the experimental errors or other undetermined factors, the present data were unable to show such a relationship.

On the basis of mineral structure, the ratios  $K(A) = \frac{x_A^{Hb}(1-x_A^{Bio})}{(1-x_A^{Hb})x_A^{Bio}}$  and  $D(A) = \frac{x_A^{Hb}}{x_A^{Bio}}$  were calculated for each major element from chemical analysis data, the results show that both values for each element are quite close to constant except for Na and Ca.

The behaviour of minor elements distributing in minerals can be considered as following the behaviour of major elements in structural sites. If a minor element substitutes for a given major element, the distribution coefficients,  $D$ , of both major and minor elements should be close. The distribution coefficients calculated from chemical and spectrographic analyses indicate that the following relations are possible:

1. Be substitutes more easily for Si than for Al in tetrahedral coordination.
2. Ga substitutes for Al in tetrahedral coordination.
3. Cr and V substitute for Al and Fe<sup>+2</sup> or Fe<sup>+3</sup> in octahedral coordination.
4. Ni and Co substitute for Mg and Fe<sup>+2</sup> in octahedral coordination.
5. Sr substitutes for Ca in 8- or 12-fold coordination.
6. Ba and Rb substitute for K in 8- or 12-fold coordination.
7. Mn probably substitute for Ca and others(?).
8. Li, Ti, Cu and Zr are of unknown behaviour.

The ionic radii of cations are generally in agreement with the possible substitutions as stated above, but in some cases such as Ga substituting for Al, and Ni and Co substituting for Mg, the electronegativity is not in conformity with the interpreted substitution.

#### REFERENCES

- Adams, F.D. and Barlow, A.E., 1910. Geology of the Haliburton and Bancroft areas, Province of Ontario (with maps No. 708 and 770). Geol. Surv. Canada, Memoir 6.
- Ahrens, L.H., 1952. The use of ionization potentials. *Geochim. et Cosmochim. Acta.*, Vol. 2, pp. 155-169.
- Bethke, P.M. and Barton, P.B., Jr., 1959. Trace element distribution as an indication of pressure and temperature of ore deposition. (Abstract), *Bull. Geol. Soc. Amer.*, Vol. 70, pp. 1569-1570.
- \_\_\_\_\_, \_\_\_\_\_ and Page, N.T., 1958. Primary experiments on the distribution of selenium between coexisting sulfides. (Abstract) *Bull. Geol. Soc. Amer.*, Vol. 69, pp. 1759-1760.
- Cloos, E., 1934. The Loon Lake pluton, Bancroft area, Ontario, Canada. *Jour. Geol.*, Vol. 42, pp. 393-399.
- Deer, W.A., Howie, R.A. and Zussman, J., 1962. Rock forming minerals. Longmans.
- DeVore, G.W., 1955a. The role of adsorption in the fractionation and distribution of elements. *Jour. Geol.*, Vol. 63, pp. 159-190.
- \_\_\_\_\_, 1955b. Crystal growth and the distribution of elements. *Jour. Geol.*, Vol. 63, pp. 471-494.
- Fleischer, H. and Stevens, R.E., 1962. Summary of new data on rock samples G-1 and W-1. *Geochim. et Cosmochim. Acta.*, Vol. 26, pp. 525-543.

- Fyfe, W.S., Turner, F.J. and Verhoogen, J., 1958. Metamorphic reactions and metamorphic facies. Geol. Soc. Amer., Memoir 73.
- Harpur, J.R., 1954. Formation of epidote in Tanganyika. Bull. Geol. Soc. Amer., Vol. 65, pp. 1075-1092.
- Hewitt, D.F. and Satterly, J., 1957. Haliburton-Bancroft area. Ontario Dept. Mines, Map, No. 1957b.
- Hietanen, A., 1956. Kyanite, andalusite and sillimanite in the schist in Boehls Butte quadrangle, Idaho. Amer. Min., Vol. 41, pp. 1-27.
- Kretz, R., 1959. Chemical study of garnet, biotite and hornblende. Jour. Geol., Vol. 67, pp. 371-402.
- \_\_\_\_\_, 1960. The distribution of certain elements among coexisting calcic pyroxenes, calcic amphiboles and biotite in skarns. Geochim. et Cosmochim. Acta, Vol. 20, pp. 161-191.
- \_\_\_\_\_, 1961. Some applications of thermodynamics to coexisting minerals of variable composition. Example: orthopyroxene-clinopyroxene and orthopyroxene-garnet. Jour. Geol., Vol. 69, pp. 361-387.
- Horham, R.L., 1965. Distribution of minor elements in coexisting hornblendes and biotites. Canadian Min., Vol. 3, Part 2, pp. 204-240.
- Muller, R.F., 1960. Compositional characteristics and equilibrium relations in mineral assemblages of a metamorphosed iron formation. Amer. Jour. Sci., Vol. 258, pp. 449-497.
- \_\_\_\_\_, 1961. Analysis of relations among Mg, Fe and Mn in certain metamorphic minerals. Geochim. et Cosmochim. Acta, Vol. 25, pp. 267-296.

- Nickel, E.H., 1954. Distribution of major and minor elements in coexisting ferromagnesian silicates. *Amer. Min.*, Vol. 39, pp. 486-493.
- \_\_\_\_\_, 1955. The distribution of major and minor elements among some coexisting ferromagnesian silicates. *Amer. Min.*, Vol. 40, pp. 699-703.
- Phinney, W.C., 1963. Phase equilibria in the metamorphic rocks of St. Paul Island and Cape North, Nova Scotia. *Jour. Petrol.*, Vol. 4, Part I, pp. 90-130.
- Prigogine, I. and Defay, R., 1954. *Chemical thermodynamics*. Longmans.
- Ramberg, H., 1949. The facies classification of rocks, a clue to the origin of quartzo-feldspathic massifs and veins. *Jour. Geol.*, Vol. 57, pp. 18-54.
- \_\_\_\_\_ and DeVore, G.W., 1951. The distribution of  $Fe^{+2}$  and  $Mg^{+2}$  in coexisting olivines and pyroxenes. *Jour. Geol.*, Vol. 59, pp. 193-210.
- Rosenqvist, I.T., 1952. *The metamorphic facies and feldspar minerals*. Universitete i Bergen Arbob, Naturv., No. 4.
- Saha, A.K., 1959. Emplacement of three granitic plutons in southeastern Ontario, Canada. *Bull. Geol. Soc. Amer.*, Vol. 70, pp. 1293-1326.
- Sahama, Th. G., 1950. *Geochemistry*. University of Chicago Press.
- Shaw, D.M., 1957. Some recommendations regarding metamorphic nomenclature. *Geol. Assoc. Canada Proc.*, Vol. 9, pp. 69-81.
- \_\_\_\_\_, 1960. The geochemistry of scapolite. *Jour. Petrol.*, Vol. 1, pp. 218-285.
- \_\_\_\_\_, 1962. *Geology of Chandos township*. Ontario Dept. of Mines, Geological Report No. 11.

- Smales, A.A., 1955. Some trace elements determinations in G-1 and W-1 by neutron activation. *Geochim. et Cosmochim. Acta.*, Vol. 8, p. 300.
- Turekian, K.K. and Phinney, W.C., 1962. The distribution of Mn, Co, Cr, Cu, Ba and Sr between biotite-garnet pairs in a metamorphic sequence. *Amer. Min.*, Vol. 47, pp. 1434-1441.
- Turner, F.J., 1948. Mineralogical and structural evolution of metamorphic rocks. *Geol. Soc. Amer.*, Memoir 30.

APPENDIX 1. Mineral composition and approximate mode of samples

(a) Almandine amphibolite facies

Sample Number	Hb	Bio	Dio	Hy	G	Scp	Ep	Q	Pl	Mc	Other Accessories	An % in Pl
# 501	10	10						78	1		cal 1, sph.	
# 503	40	35						20	5		mg	33
# 508	2	25						30	20	10	cal 2, mg 1	37
# # 703	10	40				10		35	5	few	mg	45
# # 704	10	20				5		65	few		sph, mg	
# 705	10	50				10		25	5			37
707	25					15	10	45			cal 2, sph 1, mg	
708	few	30	10*			25		30		few	mg 3, sph, Ap	
709			30*			60		5			sph 2, (mg + pyt) 3	
# 710	30	3	15*			20		30			sph	
# 711	25	20				10		40	3		sph	
712		30						35		35	mg	
713		30						30	few	40	mg	35
# 715	25	10				10		50	5		cal 1, mg	37
717		10			3			50	few	30	Muc 2, mg 3, Ap	33
# 747	15	10						65	5		cal 3, mg 2	27
# 757	15	5	25			50			5		cal	32
758 <sup>4</sup>	15	10		5*				55	10		cal 5, mg	25

# Sample of which hornblende and biotite analyzed spectrographically

# # " " " " " " " " both chemically and spectrographically

+ Probably augite

\* Hy is a relic mineral

No. 501, 503 are on Highway 504, 1/4 mile, 1 1/4 miles west of Apsley respectively.

(a) Almandine amphibolite facies (continued)

Sample Number	Hb	Bio	Dio	Hy	G	Sep	Ep	Q	Pl	Mc	Other Accessories	An % in Pl
# 761	20	20						50	10		cal 2,	26
# 770	15	20						55	5		cal 3, mg	
# 780	30	10						20	40		sph, mg	38
# 781	15	15						65	5		sph	
# 782	20	15						45	20			35
# 786	30	5						50	15		sph, mg	38
# 788	15	20				10		20		35	sph, mg	
# 789	10	15					10	50			cal 2, Al n 15, sph	

No. 770 is on Highway 504, 2 miles west of Apsley.

## (b) Hornblende hornfels facies

Sample Number	lb	Bio	Dio	Hy	G	Scp	Ep	Q	Pl	Mc	Other Accessories	An % in Pl
506	35		15					45	3		sph, mg	30
507	(1)10		15				10	60	few		sph 3, mg 2	} two layers
	(2)20		10				5	60	few		sph 2, mg 1	
# 604	2	20						60	10		cal, sph, mg	36
605	(1)	20			5			45	30		mg, cal	} two layers
	(2)25							40	few		Aln 35, sph, mg	
# 606	15	25						55	5		cal, mg	35
# 607	10	15						60	15		mg, cal	36
		20						75	3	10	cal, Zir, mg	27
		25						50	15	10	mg	26
	80	few						10	10		mg, pyt	40
	10		35					30	20		cal, sph	45
			20		5	5	10	55	few		cal 3, sph 2	
# 724	40	5						45	3		cal 2, sph 3, mg	32
		few	30					60	5		mg 4, sph 1	45
	20	25						30	10		mg 15	36
	10	few	20					65	few		cal 1, sph, mg	
# 735	50	2						35	10	few	sph 2	28
# 736	10	2	15					50	15		mg 5, sph 2	30
# 739	10	15						50	20		sph 2, mg 2, cal	30
	15		10				10	55	3	few	sph, Sp, mg	35
	10		15			5	10	50	5		cal 1, mg 5, sph	36

(b) Hornblende hornfels facies (continued)

Sample Number	Hb	Bio	Dio	Hy	G	Scp	Ep	Q	Pl	Mc	Other accessories	An % in Pl
# # 744	10	10					5	45	30		sph 1	28
745	40	20					few	35	few		mg 3, sph 1	
# 749	5	20						70	few		cal 1, sph 1, (mg + Il) 3	
750		10						55	25	5	cal, sph 1, mg 3, Zir	27
# 752	(1)10				25	5	30	30	few		cal, sph, mg	38 } two layers
	(2) 5	10						75	5		cal 2, sph 2, mg	
# # 753	10	10						60	15		cal 1, sph 1, mg 3	32
# 755	2	25						60	10		cal 1, mg 2, sph	35
# # 756	5	5					5	75	10		cal 1	32
# 791	2	20					3	60	5	10	sph	30

(c) Pyroxene hornfels facies

Sample Number	Hb	Bio	Dio	Hy	G	Scp	Ep	Q	Pl	Mc	Other accessories	An % in Pl
504		few	40		2	25		15	15		sph 1, mg 2	44
603(1)		15						45	20		cord 10, mg 10	37
603(2)		5		50				25	10		mg 10	37
726	20*			30				20	20		mg 10	50
72-200-4	5	few		30				40	15		mg 10	37

\* is an alteration product

(d) Igneous Rocks

# 514	10	15						25	45		cal, sph 3, mg 2	32
# 0904	2	3						58	24		cal 2, Neph 11, cancrinite	5

No. 514 Twin Lake diorite, Methuen township, Ontario

No. 0904 Blue Mountain nepheline-syenite, Methuen township, Ontario

Abbreviations

Aln	Allanite	Hy	Hypersthene	Q	Quartz
Ap	Apatite	Il	Ilmenite	Scp	Scapolite
Bio	Biotite	Mc	Microcline	Sp	Spheno
Cal	Calcite	Mt	Magnetite or other opaque minerals	Tom	Tourmaline
Dio	Diopside	Muc	Muscovite	Cord	Cordierite
Ep	Epidote	Pl	Plagioclase	Ura	Uralite
G	Garnet	Pyt	Pyrite		
Hb	Hornblende				

## Appendix 2. Detail of the Spectrographic Method

Spectrograph:	JACO 21 foot grating spectrograph, Wadsworth mount, first order dispersion 5.2 Å/mm.
Condensing Optics:	(distances are from the slit) 0.0 cm. Cylindrical lens (horizontal axes) Focal length 25 cm 16.1 cm. Cylindrical lens (vertical axes) Focal length 6.7 cm 27.5 cm. Diaphragm with 5 mm. aperture 58.1 cm. Spherical lens, focal length 10 cm. 72.5 cm. Arc location
Arc Gap:	4 mm.
Slit Width:	30 microns
Slit Height:	8 mm.
Intensity Reduction:	7-step rotating sector (log intensity ratio = 0.2) at the slit. Two mesh screens used for the range 2400-4800 Å, or yellow filter for the range 5700-8300 Å at the diaphragm
Voltage:	225 volts D.C., open circuit
Current:	9.5 amps.
Exposure:	samples burned to completion (50-70 seconds burning time)
Electrodes:	Anode: United Carbon Products Co. preformed 1/8" diameter rod; plain crater 1/16" x 5/8" Cathode: National Carbon Co., special graphite; 1/8" diameter rod
Gas Jet:	Stallwood jet used with a mixture of 79% Argon and 21% oxygen for the range 2400-4800 Å, or air stream for the range 5700-8300 Å at 18 SCHF.
Cooling:	Water at 15 GPH
Photographic Plates:	Eastman Kodak Type S.A.I. (range 2400-3600 Å) " " Type IIIF (range 3600-4800 Å) " " Type I-N (range 5700-8300 Å)

**Processing:**

Kodak D-19 Developer, 3 minutes at 20°C.  
Fixer, 5 minutes at 20°C.

**Photometry:**

JACO microphotometer, three steps measured,  
background set to 100 on first step read,  
correction read on third step.

Appendix 3. Analytical and standard spectral lines, and  
the range of working curves

Analytical/standard line	Range of curve (in ppm)
Ga 2943 / Pd 3242	5-1000
Be 3130 / Pd 3242	3-1000
Sn 3174 / Pd 3242	5-1000
V 3184 / Pd 3242	10-1000
Cu 3274 / Pd 3242	1-1000
Zr 3391 / Pd 3242	30- 500
Ni 3414 / Pd 3421	3-1000
Co 3453 / Pd 3421	5-1000
Sc 3911 / Cs 4555	10-1000
Mn 4041 / Cs 4555	300-30000
Sr 4077 / Cs 4555	1- 100
Cr 4254 / Cs 4555	30-1000
Ti 4305 / Cs 4555	1000-30000
Li 6103 / Cs 6723	30-3000
Li 6707 / Cs 6723	3- 100
Ba 6141 / Cs 6723	3-3000
Ba 6497 / Cs 6723	100-3000
Rb 7947 / Cs 7609	30-1000
Rb 7800 / Cs 7609	10-1000

## APPENDIX 4. Chemical Analyses\*

## Biotite of the almandine amphibolite facies

	703	704	761	788
SiO <sub>2</sub>	38.25	36.84	36.84	38.66
TiO <sub>2</sub>	1.98	3.02	3.59	1.87
Al <sub>2</sub> O <sub>3</sub>	15.04	15.37	14.75	14.25
Fe <sub>2</sub> O <sub>3</sub>	1.49	2.78	2.22	1.33
FeO	15.53	18.32	21.16	16.26
MnO	.08	.09	.32	.10
MgO	13.35	10.16	8.70	13.36
CaO	.30	.43	.46	.56
Na <sub>2</sub> O	.10	.10	.11	.12
K <sub>2</sub> O	9.66	9.45	9.11	9.63
H <sub>2</sub> O <sup>+</sup>	2.49	2.89	2.88	2.33
H <sub>2</sub> O <sup>-</sup>	.07	.05	.10	.06
Sum	98.34	99.50	100.24	98.58

## Number of ions on the basis of 24 O

Si	5.901) )8.000	5.695) )8.000	5.720) )8.000	5.983) )8.000
Al	2.099)	2.305)	2.280)	2.017)
Al	.635)	.494)	.419)	.582)
Ti	.230)	.351)	.419)	.217)
Fe <sup>+3</sup>	.173)	.323)	.259)	.161)
Fe <sup>+2</sup>	2.002)6.117	2.367)5.886	2.746)5.897	2.103)6.156
Mn	.010)	.012)	.042)	.013)
Mg	3.010)	2.339)	2.012)	3.080)
Ca	.049)	.071)	.076)	.090)
Na	.030)1.979	.030)1.963	.033)1.912	.036)2.029
K	1.900)	1.862)	1.803)	1.900)
H	2.561	2.978	2.980	2.404

\* By J. Nuysson

## APPENDIX 4 (continued)

## Biotite of the hornblende hornfels facies

	724	744	753	756
SiO <sub>2</sub>	37.80	37.93	38.65	37.84
TiO <sub>2</sub>	2.86	1.82	2.55	2.29
Al <sub>2</sub> O <sub>3</sub>	14.65	15.35	15.83	16.10
Fe <sub>2</sub> O <sub>3</sub>	2.60	3.43	2.68	2.85
FeO	16.94	13.14	12.86	14.57
MnO	.26	.30	.36	.37
MgO	11.37	13.71	13.49	12.24
CaO	.59	.81	.79	.52
Na <sub>2</sub> O	.13	.15	.23	.09
K <sub>2</sub> O	9.09	8.75	8.92	9.23
H <sub>2</sub> O <sup>+</sup>	2.88	3.83	3.12	3.30
H <sub>2</sub> O <sup>-</sup>	.02	.19	.08	.10
Sum	99.19	99.41	99.56	99.50

## Number of ions on the basis of 24 O

Si	5.808) 8.000	5.667) 8.000	5.781) 8.000	5.709) 8.000
Al	2.192)	2.333)	2.219)	2.291)
Al	.460)	.370)	.571)	.570)
Ti	.330)	.205)	.287)	.260)
Fe <sup>+3</sup>	.301)	.386)	.302)	.324)
Fe <sup>+2</sup>	2.176)5.903	1.641)5.691	1.608)5.820	1.838)5.754
Mn	.034)	.038)	.046)	.047)
Mg	2.602)	3.051)	3.006)	2.751)
Ca	.097)	.129)	.127)	.084)
Na	.039)1.917	.043)1.839	.064)1.893	.026)1.886
K	1.781)	1.667)	1.702)	1.776)
H	2.949	3.815	3.111	3.319

## APPENDIX 4(continued)

## Hornblende of the almandine amphibolite facies

	703	704	761	788
SiO <sub>2</sub>	41.97	40.46	42.25	42.38
TiO <sub>2</sub>	.58	.90	1.44	.64
Al <sub>2</sub> O <sub>3</sub>	12.70	12.92	10.91	11.56
Fe <sub>2</sub> O <sub>3</sub>	4.23	7.11	3.98	4.27
FeO	13.64	14.42	17.09	13.88
MnO	.13	.14	.49	.17
MgO	9.49	7.47	8.37	9.66
CaO	11.48	11.14	10.20	11.55
Na <sub>2</sub> O	.85	1.18	1.26	1.31
K <sub>2</sub> O	1.99	1.67	1.37	1.75
H <sub>2</sub> O+	1.66	1.54	2.16	1.31
H <sub>2</sub> O-	.03	.03	.05	.02
Sum	98.75	98.98	99.57	98.50

## Number of ions on the basis of 24 O

Si	6.322) )8.000	6.236) )8.000	6.425) )8.000	6.510) )8.000
Al	1.678)	1.764)	1.575)	1.490)
Al	.629)	.582)	.379)	.604)
Ti	.068)	.105)	.164)	.074)
Fe <sup>+3</sup>	.491)	.824)	.455)	.494)
Fe <sup>+2</sup>	1.757) 5.142	1.858) 4.998	2.173) 5.130	1.782) 5.197
Mn	.017)	.019)	.063)	.022)
Mg	2.180)	1.715)	1.896)	2.211)
Ca	1.895)	1.838)	1.661)	1.901)
Na	.254) 2.540	.353) 2.520	.371) 2.298	.390) 2.634
K	.391)	.329)	.266)	.343)
H	1.706	1.582	2.189	1.341

## APPENDIX 4 (continued)

## Hornblende of the hornblende hornfels facies

	724	744	753	756
SiO <sub>2</sub>	42.63	42.80	43.74	42.25
TiO <sub>2</sub>	.91	.73	1.11	1.22
Al <sub>2</sub> O <sub>3</sub>	11.17	10.78	10.72	11.53
Fe <sub>2</sub> O <sub>3</sub>	6.34	7.18	6.23	6.51
FeO	13.19	11.11	10.19	12.02
MnO	.42	.43	.63	.57
MgO	9.14	10.53	11.60	9.73
CaO	11.26	11.39	11.09	11.25
Na <sub>2</sub> O	1.36	1.41	1.18	1.21
K <sub>2</sub> O	1.26	1.31	1.02	1.40
H <sub>2</sub> O+	1.55	1.66	1.84	1.57
H <sub>2</sub> O-	.02	.00	.00	.00
Sum	99.25	99.32	99.35	99.26

## Number of ions on the basis of 24 O

Si	6.481) 8.000	6.456) 8.000	6.509) 8.000	6.400) 8.000
Al	1.519)	1.544)	1.491)	1.600)
Al	.481)	.372)	.329)	.453)
Ti	.104)	.082)	.124)	.139)
Fe <sup>+3</sup>	.725)	.814)	.697)	.741)
Fe <sup>+2</sup>	1.676) 5.110	1.401) 5.088	1.267) 5.128	1.522) 5.128
Mn	.054)	.055)	.080)	.073)
Mg	2.070)	2.364)	2.571)	2.195)
Ca	1.833)	1.840)	1.768)	1.825)
Na	.401) 2.479	.412) 2.504	.341) 2.303	.355) 2.450
K	.245)	.252)	.194)	.270)
H	1.570	1.669	1.825	1.536

APPENDIX 5. Spectrographic Analyses (averages of triplicates)

	Sn ppm	Be ppm	Ga ppm	Ti ppm	Cr ppm	V ppm	Li ppm	Ni ppm	Co ppm	Cu ppm	Mn ppm	Sc ppm	Zr ppm	Sr ppm	Ba ppm	Rb ppm
501B	-	3	61	9550	tr	132	550	12	29	37.2	2500	57	93	7.4	225	765
503B	-	11.8	69	13700	640	503	92	330	54	4.5	1630	tr	79	tr	1100	360
508B	-	6.6	74	17250	73	587	121	15	91	10.5	2180	tr	180	tr	560	445
604B	-	8	82	10750	74	400	150	76	73	8.8	2480	26	103	1	965	635
606B	-	4.9	56	10900	128	272	59	81	61	5.1	2520	9	96	tr	2600	595
607B	-	7.6	38	16800	20	315	235	28	40	6.7	2300	20	175	1.2	1250	520
703B	-	4.9	41	15800	113	200	265	55	44	6.6	490	tr	48	1.5	220	455
704B	-	11.3	68	18300	233	525	255	120	77	9.2	430	tr	99	1.2	104	375
705B	-	8.4	23	14200	52	410	105	43	29	10	1040	5	56	4.5	480	350
710B	-	4.5	49	8100	89	190	460	97	45	9.1	580	-	77	3.5	223	730
711B	-	7.3	48	19000	230	330	220	150	80	11	600	-	82	1	335	435
715B	-	5.4	38	15600	320	260	255	106	58	4.4	850	-	68	2.3	1150	405
724B	-	5.7	40	19500	155	330	122	101	57	5.5	1820	-	97	tr	2200	275
735B	-	9.4	41	15300	195	395	585	200	107	?	1420	-	106	5.4	355	605
736B	-	7.2	37	17400	145	295	235	160	160	260	2430	5	122	9.4	2800	615
739B	-	5.9	66	18500	89	275	320	71	68	22	2520	3	86	2	1580	545
744B	-	7.4	118	13100	132	305	230	114	92	35	2450	tr	78	6.2	1130	640
747B	-	5.6	123	12900	tr	315	63	70	75	28	1780	3	200	2.8	1330	460
749B	-	5.4	48	10500	145	270	163	119	79	4.9	2500	31	67	1	1000	695
752B	-	8.1	50	14300	125	200	117	44	81	7.5	2380	195	137	2.9	3120	490

APPENDIX 5 (continued)

	Sn ppm	Be ppm	Ga ppm	Ti ppm	Cr ppm	V ppm	Li ppm	Ni ppm	Co ppm	Cu ppm	Mn ppm	Sc ppm	Zr ppm	Sr ppm	Ba ppm	Rb ppm
753B	-	5	40	14700	60	242	118	73	77	6.6	2670	16.6	66	7.4	1900	370
755B	17	5.6	66	10400	110	295	118	101	75	4.1	2600	12	83	2.1	2520	615
756B	11.5	5.5	70	12700	122	240	106	101	75	8.2	2780	3	60	2.3	1100	440
757B	20	4.9	125	6300	107	200	155	78	83	145	490	-	101	23	1280	680
761B	29	9.3	85	16300	tr	490	105	27	94	60	2330	-	160	1.1	1250	475
770B	tr	8	39	5800	82	340	85	54	110	16	2300	-	106	1.4	2180	400
780B	tr	4.6	74	5800	315	250	155	275	103	75	1020	-	71	7.1	1300	435
781B	-	5.7	45	17500	112	240	350	120	72	21	1950	tr	105	1	1060	655
782B	-	4.2	49	3800	165	160	135	245	99	7	1800	tr	101	1.5	1110	500
786B	-	4	46	10500	154	207	235	165	107	40	2650	-	63	4.8	560	505
788B	-	5.7	33	11200	115	245	380	83	33	6.4	540	tr	52	tr	132	875
789B	-	4.7	19	11900	140	225	170	73	37	31	710	tr	74	2.1	245	280
791B	-	tr	65	9500	118	300	127	100	74	74	2650	tr	112	tr	440	360
904B	-	7.4	46	5900	tr	310	650	44	49	42	3100	2	117	3.4	130	890
514B	-	3.8	69	8600	tr	215	78	20	76	35	2500	-	109	2.9	1720	465
501H	tr	5.8	36	4600	26	140	20	5.7	19	13.5	4850	60	93	66	20	11.2
503H	25	11.5	23	4750	625	640	11	167	36	16.5	5000	94	82	2.1	20	tr
508H	10	6.2	45	10500	tr	323	10.6	5.7	70	18.3	4400	86	190	8.9	30	11
604H	27	14.8	33	8500	81	330	36	37.5	44	20	5600	235	135	26	35	7.4

## APPENDIX 5 (continued)

	Sn ppm	Be ppm	Ga ppm	Ti ppm	Cr ppm	V ppm	Li ppm	Ni ppm	Co ppm	Cu ppm	Mn ppm	Sc ppm	Zr ppm	Sr ppm	Ba ppm	Rb ppm
606H	13	9.8	27	5450	103	240	15.5	34	27	4.2	4950	185	115	13.3	102	5.4
607H	20	14.5	27	6400	20	250	18.5	10.3	24	3.5	4300	101	110	37	36	6.7
703H	12	8	37	3020	110	430	26	27.5	24	8.4	930	51	100	32	20	8.5
704H	-	16.2	46	3500	158	415	25	45	40	24	990	27	89	42	50	6
705H	-	7.8	24	5000	88	513	23	17.2	16	8	2100	131	59	97	25	6.3
710H	-	6.7	31	5300	125	230	47	51	30	9.2	1060	60	130	21.2	tr	7
711H	-	10.1	29	6600	290	385	45	70	46	2.9	1170	108	125	33	20	12.5
715H	-	7.9	30	7300	240	335	69	60	37	2.4	1520	51	71	22.5	51	17
724H	-	8.7	24	10700	155	330	17.5	61	48	2.9	3080	86	130	6.7	125	5.5
735H	123	34.5	25	4100	220	385	58	100	61	20	2320	71	82	21	40	12
736H	24	7.5	27	7700	178	265	37	85	86	37	3900	158	87	27	150	10.5
739H	18	11.6	35.5	10600	108	357	69	37	34.5	10.5	3650	165	104	14	58	8.6
744H	-	12.3	25	7500	170	305	31	56	44	2.7	3530	150	100	18.2	42	7.6
747H	14	13	53	11600	tr	308	4.7	32	37	21	3500	34	130	53	60	8.5
749H	9	7.2	30.8	5300	115	270	26	83	61	7.5	4270	165	135	10.3	43	4.9
752H	8	9.2	40	10200	67	220	23	29	34	5.8	4600	105	81	7.5	115	6.7
753H	8.1	9.6	24	7300	55	175	25	37	39	3	4930	112	65	23.5	72	4
755H	28	8.8	49.5	7000	103	310	30	61	46	9.7	5800	135	155	24	52	4.7
756H	46	25	60	4000	140	195	15.5	71	54	4	4700	28	74	21	53	7.6
757H	15	4.2	39	6200	130	250	10.3	31.5	36	29	960	36	44	33	56	14.5

## APPENDIX 5 (continued)

	Sn ppm	Be ppm	Ga ppm	Ti ppm	Cr ppm	V ppm	Li ppm	Ni ppm	Co ppm	Cu ppm	Mn ppm	Sc ppm	Zr ppm	Sr ppm	Ba ppm	Rb ppm
761H	tr	13.2	53	1950	tr	660	25.5	tr	52	40	3900	20	185	29	69	15.5
770H	tr	12	79	1980	89	400	10.8	tr	55	8.3	4150	54	175	22	53	6.4
780H	tr	7.2	27	7300	345	370	12.3	121	44	20	2120	52	59	27	35	6.1
781H	tr	8.4	35	2950	125	255	49	84	43	46	3600	49	58	20	45	8
782H	10	6.2	23	8150	170	340	10.8	82	45	2.5	2700	90	69	19	56	10.4
786H	tr	6.3	35	3400	165	265	35.5	100	57	3.1	5200	58	80	16	34	7.4
788H	8.1	9.5	30.5	4700	155	420	37	48	22	3	990	190	68	11	10	11
789H	9	8.7	26	4050	160	290	18.5	47	25	7.4	1450	22	87	25	10	11.3
791H	19	24	49	5350	110	360	25	32	31	18	4400	140	120	9.2	42	7
904H	24	112?	93	800	tr	255	77	7.2	18	5.5	6000	17	415	14.5	20	18
514H	14	40?	46	7950	tr	260	16.8	7.8	32	13.2	4800	117	83	57	83	8.4